LONG VALLEY OBSERVATORY QUARTERLY REPORTS
COMBINED January – December 2009

Long Valley Observatory
U.S. Geological Survey
Volcano Science Center, MS 910
345 Middlefield Rd., Menlo Park, CA 94025

http://lvo.wr.usgs.gov

LONG VALLEY OBSERVATORY QUARTERLY REPORTS
January – December 2009

CONTENTS

SUMMARY FOR 2009

The relative quiescence in Long Valley caldera and vicinity that began in the spring of 1998 continued through 2009. Earthquake activity within the caldera remained low with the largest earthquake just a M=2.7. The number of small ($M \geq 0.5$) earthquakes beneath Mammoth Mountain increased in May, and by the end of the year exceed the number of earthquakes within the caldera itself. Of particular note was a swarm of over 50 small ($M \leq 0.5$) earthquakes centered at depth of 20 to 25 km just southwest of Mammoth Mountain. The resurgent dome, which essentially stopped inflating in early 1998 and showed minor subsidence (of about 1 cm) through 2001, was followed by gradual inflation through 2002. The deformation pattern since 2003 has been characterized by gradual subsidence through early 2007 followed by renewed slow inflation through early 2010. The center of the resurgent dome remains some 75 cm higher than prior to the onset of unrest in 1980. Carbon dioxide emissions around Mammoth Mountain continue to fluctuate with measurement in the Horseshoe Lake area varying between 50 and 100 tons/day. Isolated areas of low CO_2 emission rates within the caldera (Basalt Canyon, Shady Rest, and the resurgent dome) continue to produce between 5 and 10 tons/day. Repeat measurements of CO_2 flux sites on the Mono Craters shows that the North Coulee continues to produce about 9 tons/day with an isotopic composition essentially the same as that for Mammoth Mountain. Variations in the hydrologic monitoring data are dominated by seasonal variations in precipitation showing no clear evidence of increased thermal input beneath the caldera. The thermal springs in Hot Creek continue to show variability in discharge temperatures and vent locations with subdued, infrequent geysering.

Up-to-date plots for most of the data summarized here are available on the Long Valley Observatory web pages (http://volcanoes.usgs.gov/lvo).

EARTHQUAKES *(D.P. Hill and A.M. Pitt)*

REGIONAL

Earthquake activity in the Long Valley Caldera–Mono Basin–White Mountains region during 2009 included just eight earthquakes with magnitudes M ≥ 3.0 (Figures S1 and S2). The largest of these was a M=3.7 earthquake on August 30 at 11:21 AM (DPT) located near the southwesterern end of the Adobe Hills (~ 20 km ESE of Mono Lake). The Sierra Nevada block south of the caldera continued to be the most prolific source of seismic activity in region producing five earthquakes with magnitudes between M=3.1 and M=3.3 and a host of smaller events, most of which were concentrated in the sub-parallel NNE-trending lineations that have persisted since the late 1970's. Two additional M>3 earthquakes in the region included a M=3.1 event beneath the Volcanic Tablelands on April 14 and a M=3.3 event on August 3 located 8 km west of Mount Tom along the southern margin of the area shown in Figure S1.

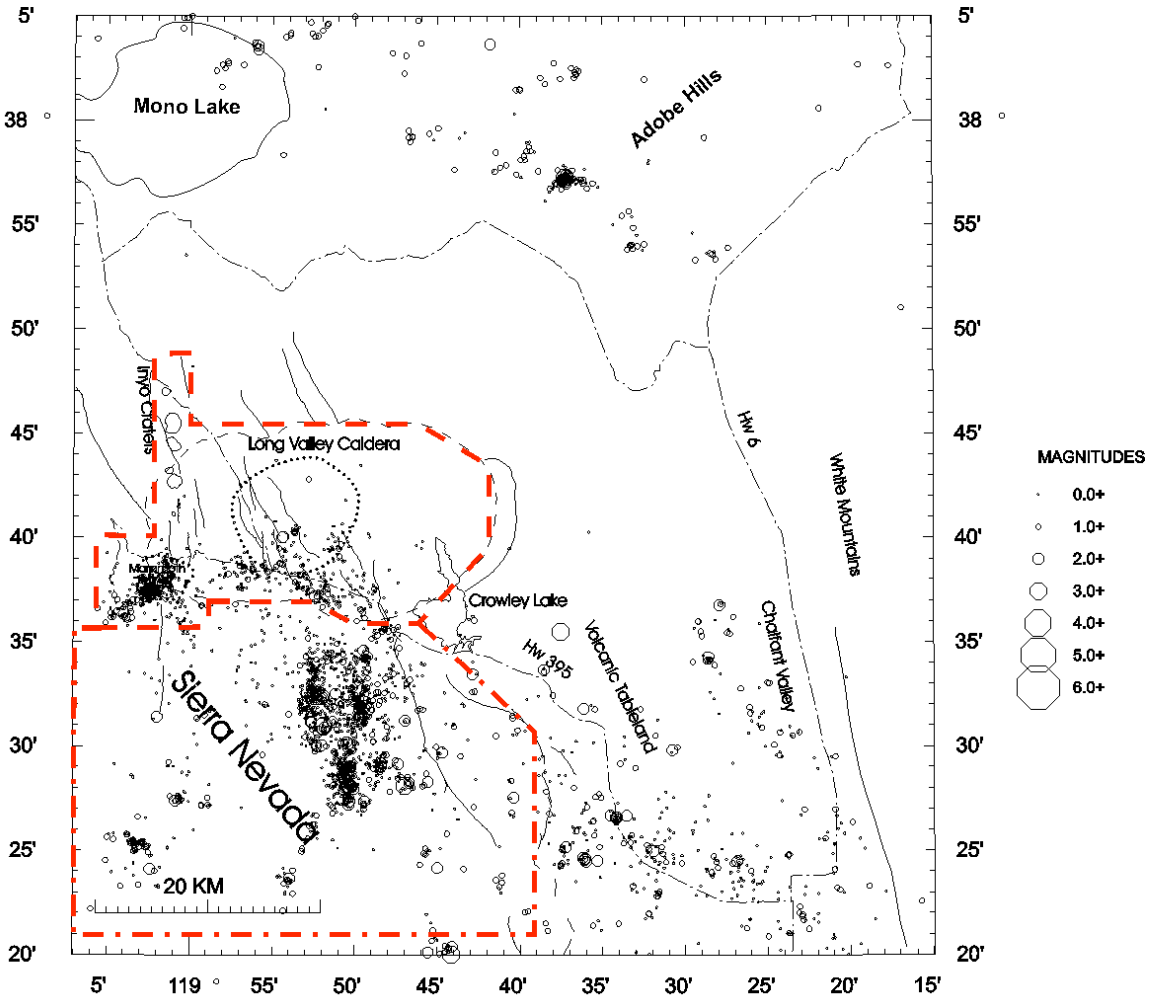

Figure S1: Earthquake epicenters in the Long Valley Caldera region: 2009
Symbol size proportional to earthquake magnitude. Dashed and dash-dot red lines outline epicenters included in the Long Valley Caldera and Sierra Nevada seismicity-time plots, respectively, in Figure S2.

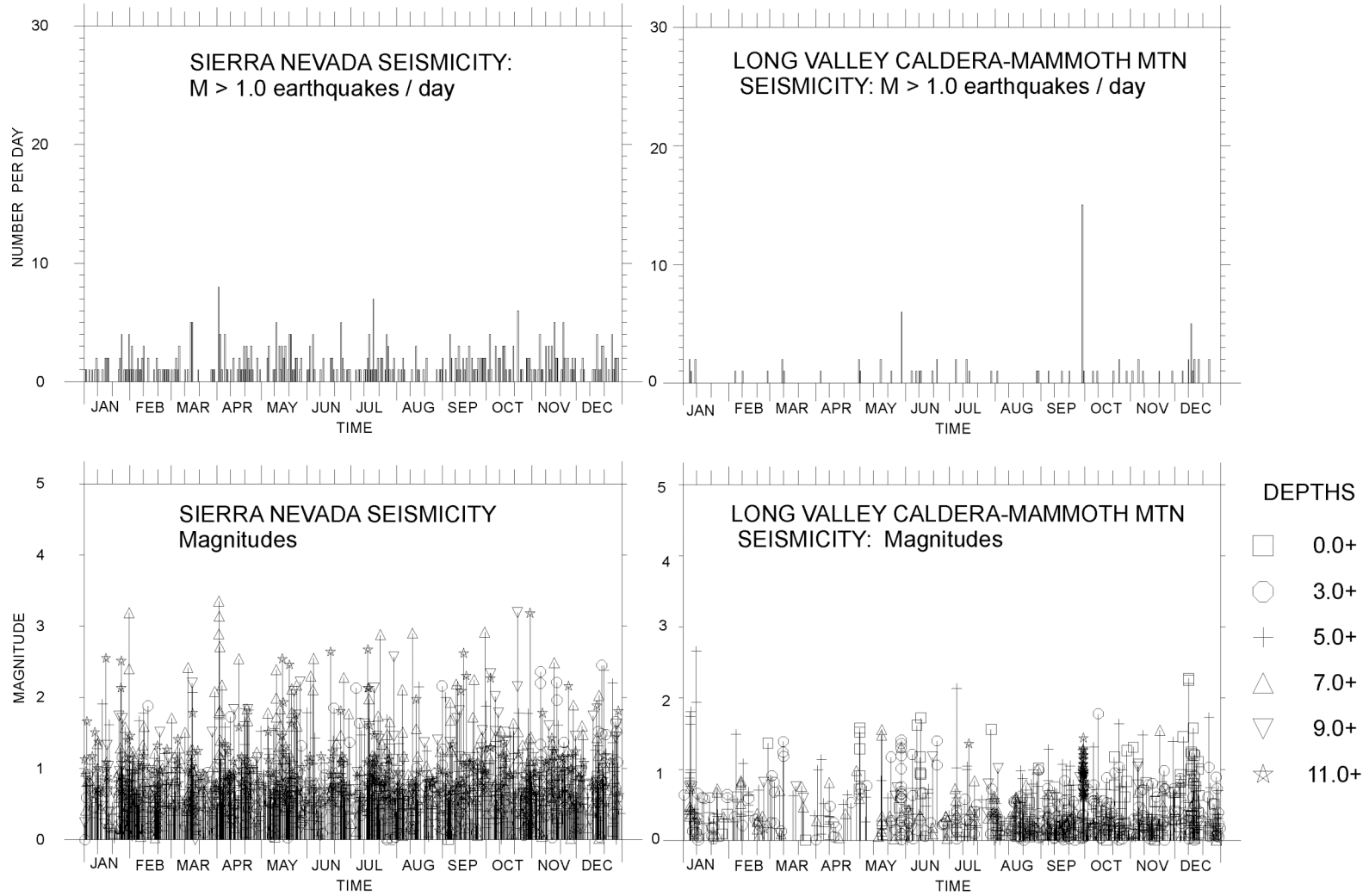

Figure S2: Temporal occurrence of earthquakes in the Sierra Nevada block south of the caldera (left) and within the Caldera and including Mammoth Mountain (right) for 2009. Top: number of M > 1.0 earthquakes per day. Bottom: earthquake magnitudes and range of focal depths (indicated in km by symbols in legend to the right).

LONG VALLEY CALDERA

Activity within Long Valley Caldera proper remained low through 2009 with just three earthquakes exceeding M=2.0. A M=2.7 earthquake on January 9 was located in the south moat near the evaporation pond (2 km SW of the airport), and a pair of M=2.3 earthquakes on December 10 were located beneath the resurgent dome (2.4 km NNW of the geothermal plant). Most of the remaining smaller earthquakes were scattered beneath the south moat and the southern half of the resurgent dome (Figures S1- S5), the same areas that produced most of the seismic activity within the caldera beginning in 1980.

MAMMOTH MOUNTAIN

The rate of small earthquakes beneath Mammoth Mountain began to increase in late May and continued at an accelerated pace through the end of 2009 (Figures S6, S7). The bulk of activity was clustered beneath the southwest flank of the mountain at a depth of ~ 5 km beneath the mean surface elevation of ~2,700 m above sea level, although a number of small earthquakes were located at depths less than 2 km (Figure S6). Many of these earthquakes occurred in rapid-fire sequences (spasmodic bursts) with multiple events occurring within time intervals ranging from tens of seconds to a few minutes. With the exception of a M=2.1 event on July 5, all of the Mammoth Mountain earthquakes had magnitudes less than M=2.0.

Of particular note was a swarm of over 50 M $\geq$ 0.5 earthquakes on September 29 located at depths of 20 to 25 km beneath an area just southwest of Mammoth Mountain between Mammoth Pass and the site of the basaltic eruptions some 8,000 years ago that formed Red Cones. As with the similar but somewhat deeper swarm (depths 25 to 35 km) of June 16, 2006, these earthquakes are distinctly deeper than the 10- to 25-km deep long-period (LP) "volcanic" earthquakes that developed during the 1989 Mammoth Mountain earthquake swarm, and which have continued sporadically through the present (the single deep LP earthquake detected in 2009 occurred on July 31). The deep earthquakes in the swarm of September 29 all had the high-frequency character of brittle-failure earthquakes similar to those occurring at depths less than 10 km. As with the deep earthquake swarm of June 2006, we suspect that these brittle-failure earthquakes are occurring within the mafic lower crust (which can remain in the brittle domain to temperatures as high as ~700^{o} C). The LP earthquakes at depth between 10 and 20 km are presumably occurring within a more silicic section of the crust which, at temperatures of ~350 to 400^{o} C, has a transitional rheology between brittle and plastic behavior. It's worth recalling that a swarm of deep, brittle-failure earthquakes spanning the same depth range occurred beneath the Sierra Nevada crest in the vicinity of Lake Tahoe in late 2003, which Smith et al., (*Sciencexpress*, 5 August 2004) concluded was associated with a magmatic intrusion in the lower crust. We, however, see no clear evidence for a significant intrusion associated with these deep swarms of brittle-failure earthquakes beneath Mammoth Mountain.

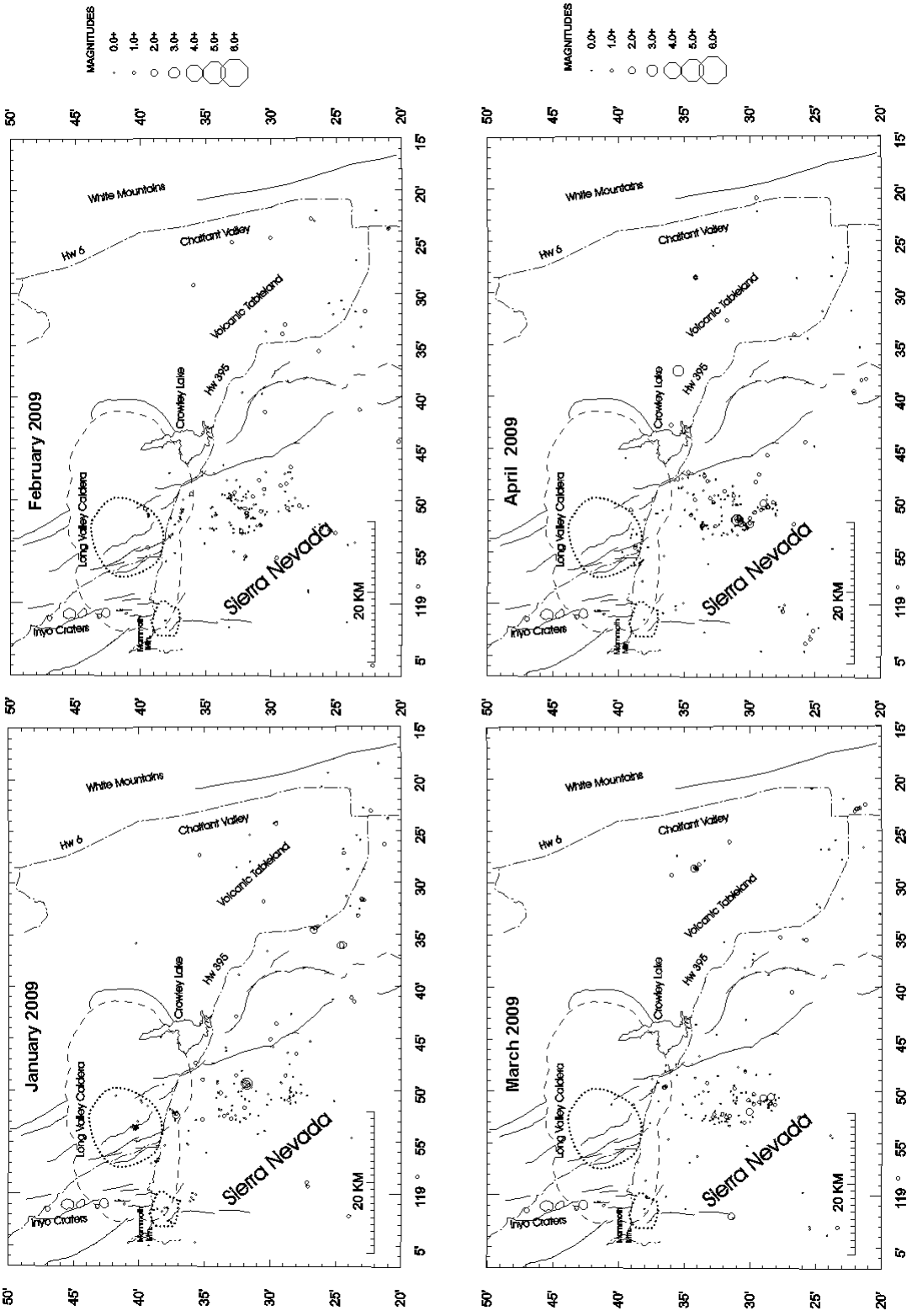

Figure S3: Earthquake epicenters in the Long Valley Caldera-Sierra Nevada region: January-April 2009

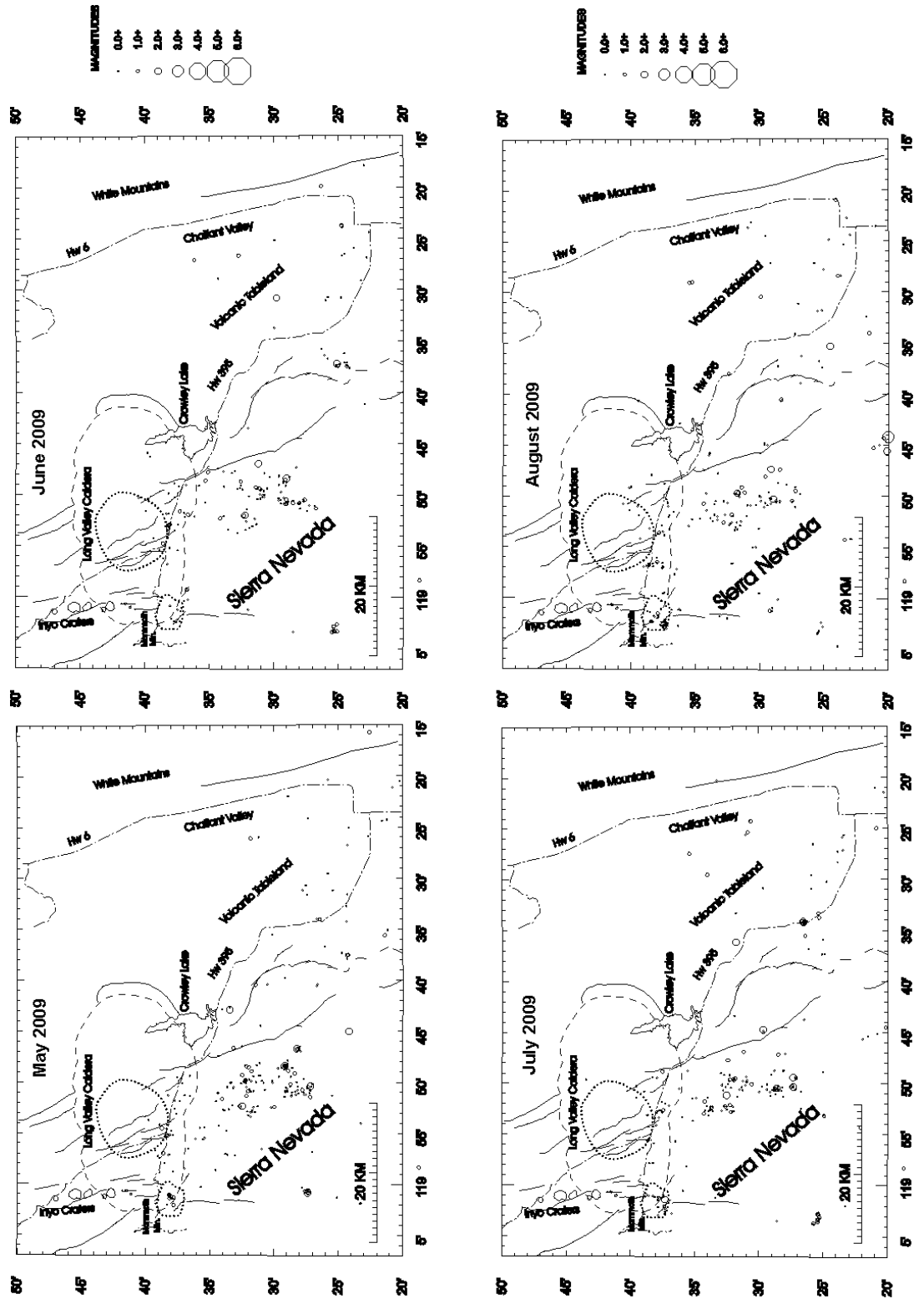

Figure S4: Earthquake epicenters in the Long Valley Caldera-Sierra Nevada region: May - August 2009

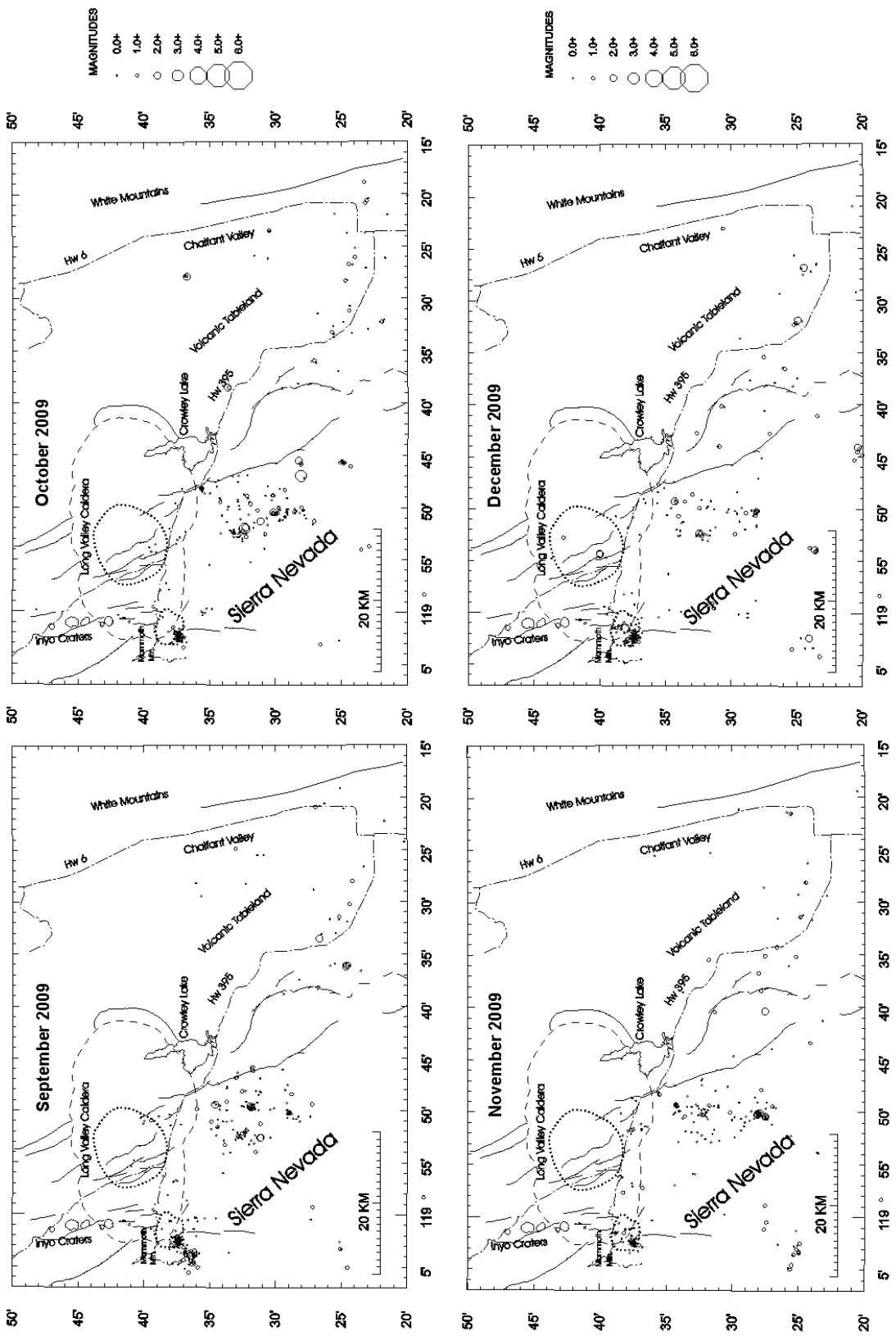

Figure S5: Earthquake epicenters in the Long Valley Caldera-Sierra Nevada region: September-December 2009

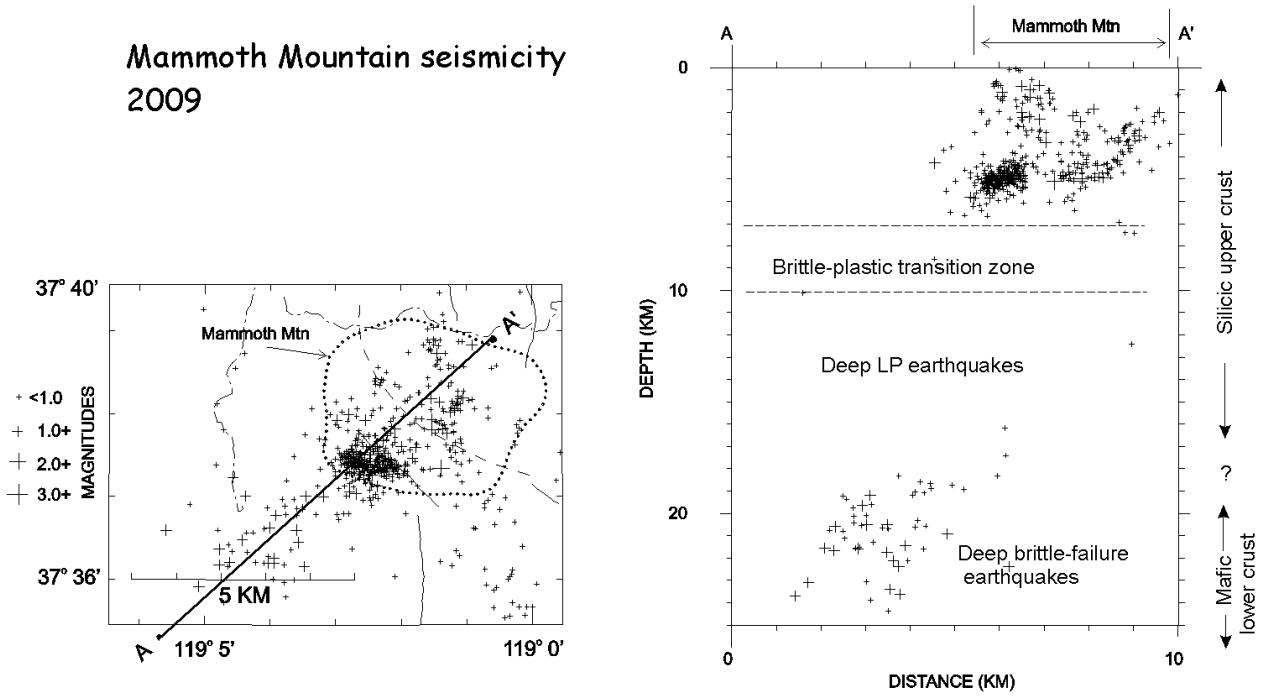

Figure S6: Map and cross section showing distribution of M>0.5 earthquakes beneath Mammoth Mountain for 2009

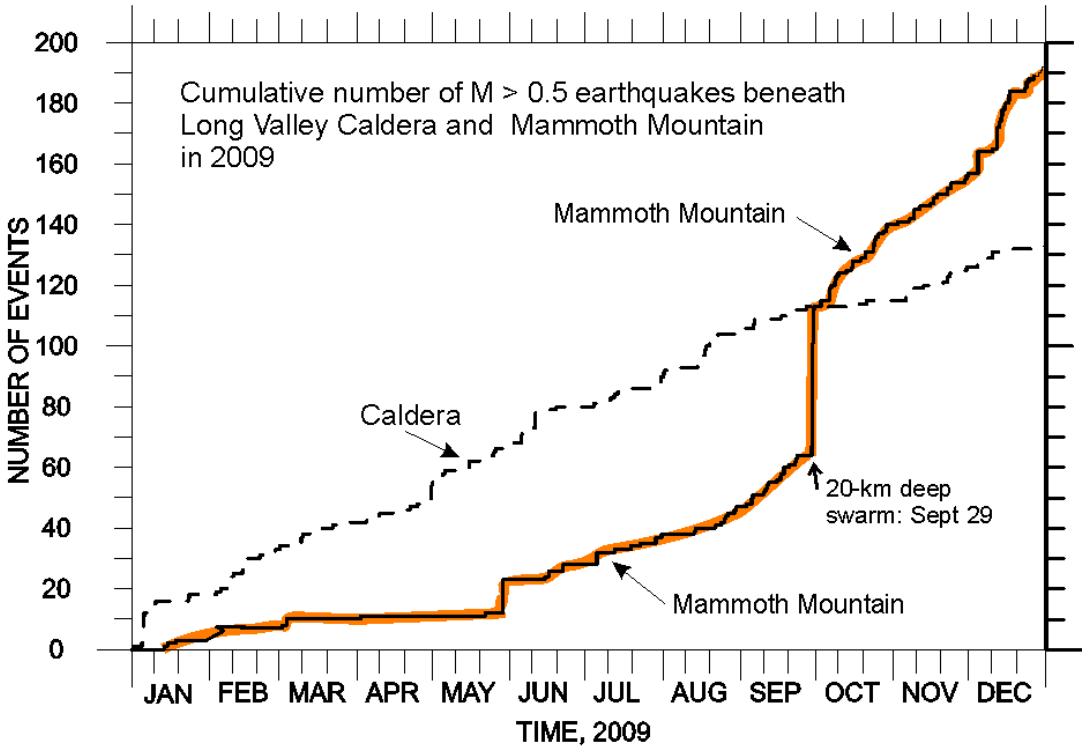

Figure S7. Cumulative number of M>0.5 earthquakes within Long Valley Caldera (dashed line) and Mammoth Mountain (solid orange line) for 2009.

MONO BASIN "TREMOR"

Beginning in early 2009, we identified episodically recurring signals with the appearance of volcanic tremor on several seismic stations in the Mono Basin. The energy in these tremor-like signals is concentrated in the 0.8 and 1.2 Hz frequency band with durations of several hours. These signals clearly stand out in spectrograms as bright (high-amplitude) bands centered at ~ 1.0 Hz on short-period, vertical-component seismic stations LUL, SLK, and MCC operated by the Seismological Laboratory at the University of Nevada, Reno (UNR), and jointly recorded by UNR and the USGS (Figure S9). It soon became evident that these signals were correlated with periods of high wind and thus were probably not an indication of renewed volcanic activity in the Mono Basin. In an effort to understand how wind might couple into the ground to mimic volcanic tremor, we co-located two temporary, 3-component instrument packages the permanent short-period stations, LUL and SLK (Figure S8) from June 10 to September 2. The three components included the vertical and one horizontal component from a STS-2 broadband seismometer (with the horizontal component oriented toward Mono Lake) plus an acoustic infrasound channel. This deployment was designed to test the possibilities that tremor-like signal was the result of 1) downward propagation of infrasound generated by turbulent "mountain waves" as high winds blow across the steep eastern escarpment of the Sierra crest, or perhaps 2) wave action on the shore of Mono Lake generating local Rayleigh waves that propagate outward from Mono Lake. Results from this experiment are pending. We feel it's important to understand the nature of this Mono Basin "tremor" so that we can distinguish future occurrences from the onset of true volcanic tremor that may portend a volcanic eruption in the basin. (The most recent eruptions in Mono Basin occurred just 250 and 600 years ago from vents on Paoha Island in Mono Lake and Panum dome at the north end of the Mono Craters volcanic chain.)

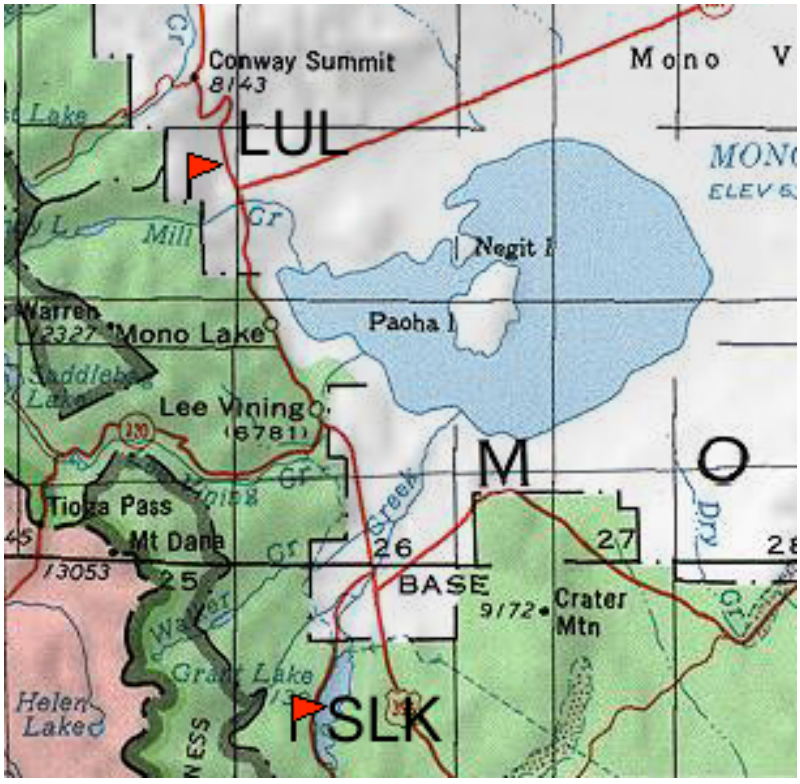

Figure S8: Map Mono Lake and the Mono Basin with locations of the temporary seismic/infrasound installations at LUL and SLK.

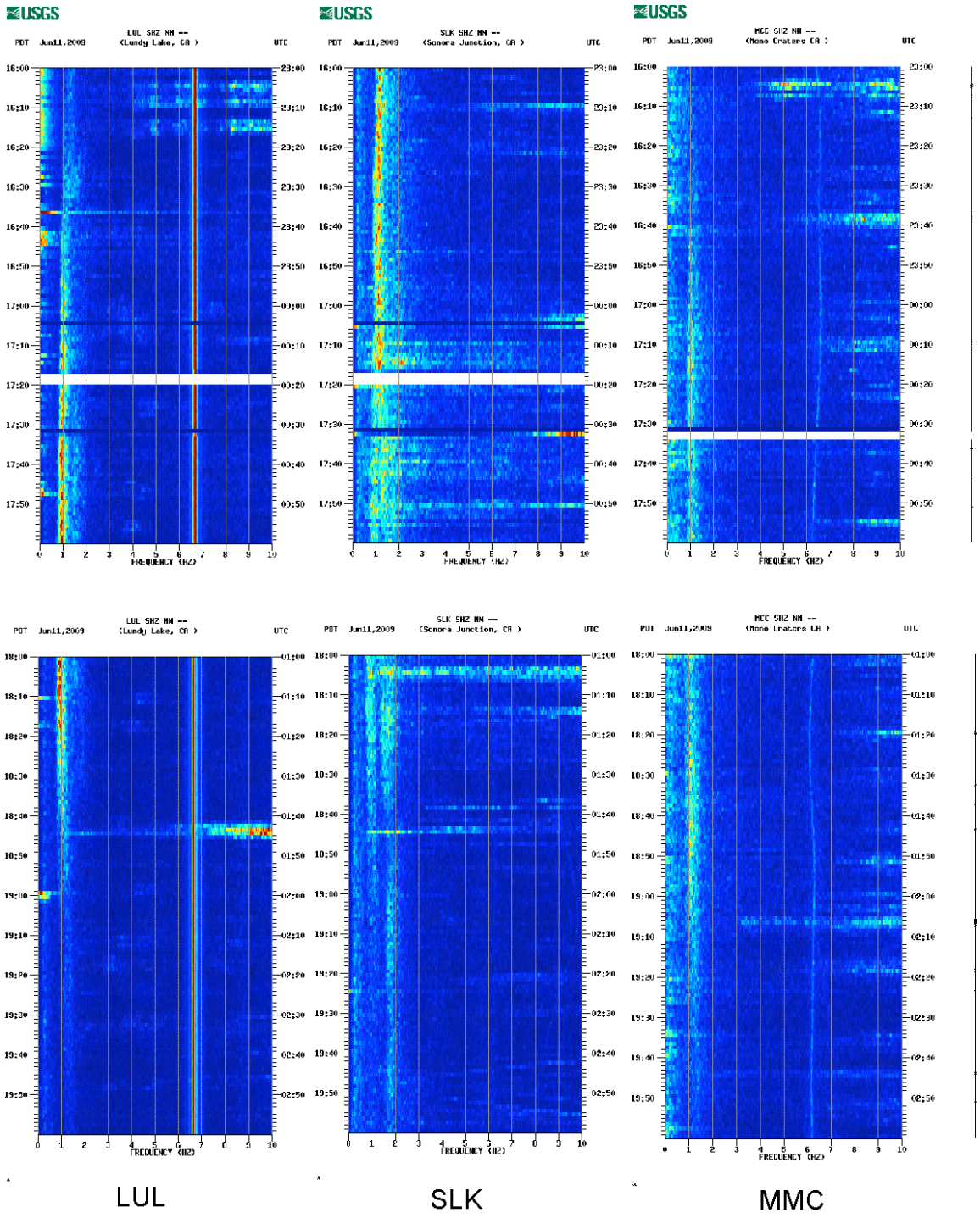

Figure S9. Examples of spectrograms recorded by the seismic stations LUL, SLK, and MMC during an episode of Mono Basin "tremor" on 11 June 2009 between 16:00 and 20:00 hours (PDT). Time in hours from 16:00 to 20:00 (PDT) on the vertical axes and frequency from 0 to 10 Hz on the horizontal axes. Increasing spectral amplitudes indicated as colors grade from blue through red.

DEFORMATION

LONG VALLEY GPS NETWORK: John Langbein, Mike Lisowski, Jessica Murray-Moraleda, Jerry Svarc, Stuart Wilkinson, and Peter Cervelli

The summary of continuous GPS measurements since January 2007 indicates: 1) Slow inflation of the resurgent dome; 2) problems in the past 6 months with updating our processing of these data. We have recently initiated processing in "real-time" 1-second samples from a subset of GPS sites with the goal of incorporating this data stream into the real-time, on-line system for monitoring volcanic unrest in the caldera.

Data examined are from 16 stations in and around the caldera operated by CVO, another 6 stations in and around the caldera operated by UNAVCO as part of PBO, and two stations (cmbb, musb) operated by UCB on the west side of the Sierras; these two stations provide a simple reference frame to interpret displacements measured at the other 22 stations.

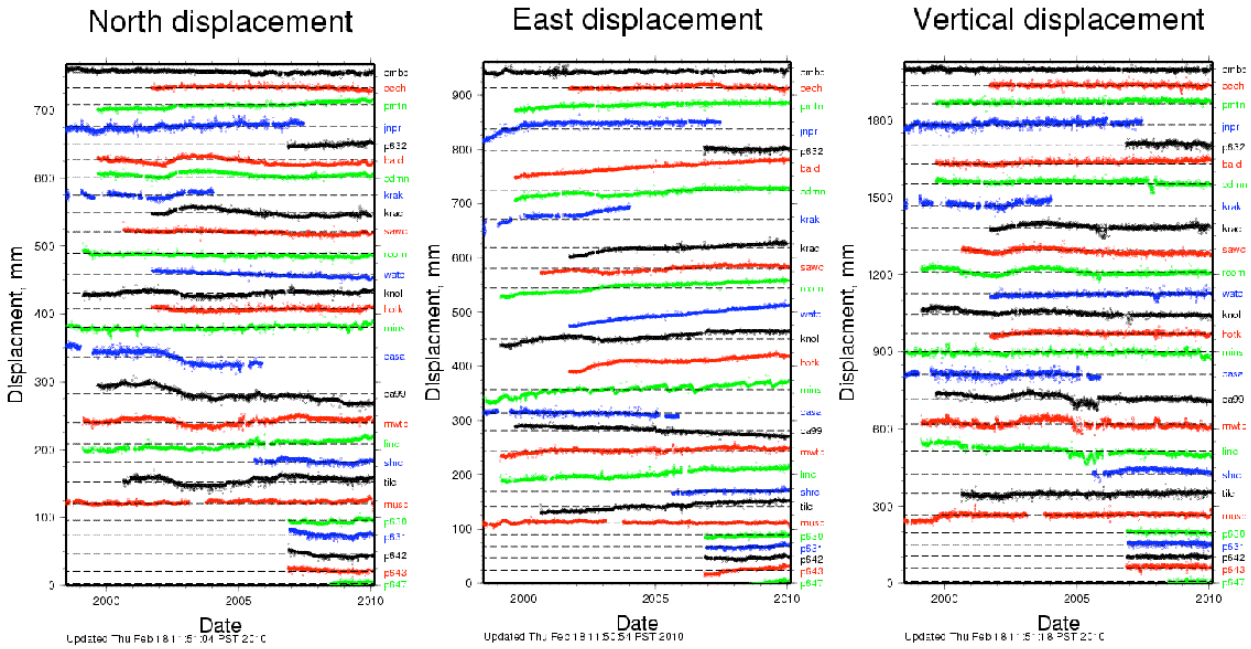

Plots of the displacement data (relative to cmbb/musb) are shown above (and on the web at: http://quake.wr.usgs.gov/research/deformation/twocolor/lv_continuous_gps.html)

In the context of the previous measurements from two-color EDM and leveling, a plot showing the baseline length changes between CASA and KRAK derived from 1982-2010 is shown as the dark blue line in Figure 2.

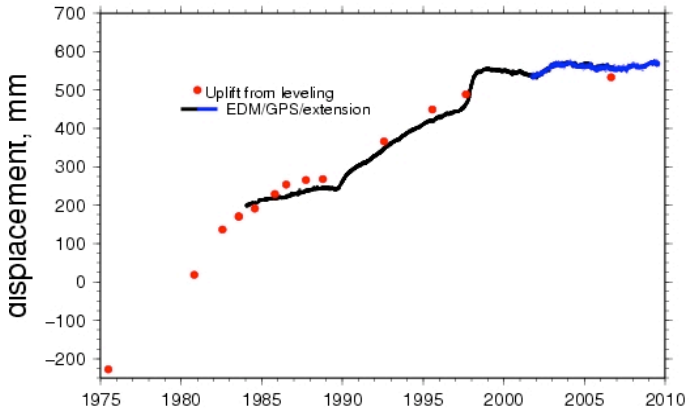

Figure 2: EDM/GPS extension CASA-KRAK compared with uplift from leveling

Examination of Figure 2 (and principle component analysis and modeling) suggests that the resurgent dome has been slowly inflating since 2007.0. The pattern of displacements since 2007 is shown in Figure 3. To first order, the displacement vectors show slow expansion, less than 5 mm/yr, centered around the resurgent dome. There are exceptions, notably, DECH and MINS.

During the past year, we have purchased software to process GPS data in "real-time" yielding estimates of position changes every second. Currently, we are processing 5 sites; the displacements of RDOM, TILC, CA99/CASA, and SHRC are being estimated relative to MWTP. All of these sites are on local, radio telemetry. In addition, we are also processing some of the PBO/UNAVCO sites that use commercial, "CDMA telemetry". Initial analysis suggests that these high rate data have repeatability on the order of 1-cm in the horizontal for these 1-second samples (For comparison, the repeatability is 1 mm for the GPS data that is processed in daily batches.)

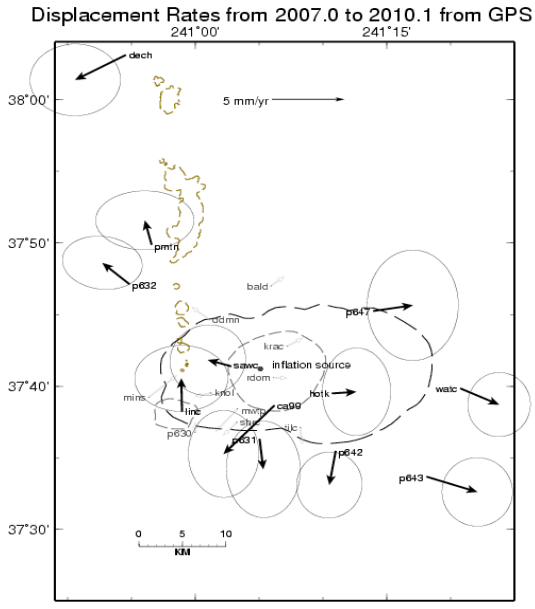

Figure 3: Displacement rates for the interval between 2007 and 2010 relative to cmbb/musb on the western slope of the Sierra Nevada. Error ellipses are "2-sigma" confidence level. Gray vectors indicate insignificant displacement rate.

CONTINUOUS BOREHOLE STRAIN MEASUREMENTS (Malcolm Johnston, Doug Myren, and Stan Silverman)

Instrumentation

Dilational strain measurements are being recorded continuously at the Devil's Postpile (POP), Motorcross (MCX) near the western moat boundary in the south moat, Big Springs (BSP) just outside the northern caldera boundary, and at

Phillips (PLV1), just to the north of the town of Mammoth Lakes. The site locations are shown in Figure D1. The instruments are Sacks-Evertson dilational strain meters and consist of stainless steel cylinders filled with silicon oil that are cemented in the ground at a depth of about 200m. Changes in volumetric strain in the ground are translated into displacement and voltage by a expansion bellows attached to a linear voltage displacement transducer. This instrument is described in detail by Sacks et al.(*Papers Meteol. Geophys*. ,22, 195, 1971).

Data from the strainmeters are transmitted using satellite telemetry every 10 minutes to a host computer in Menlo Park. The data are also transmitted with 24-bit seismic telemetry together with 3-component seismic data to Menlo Park.

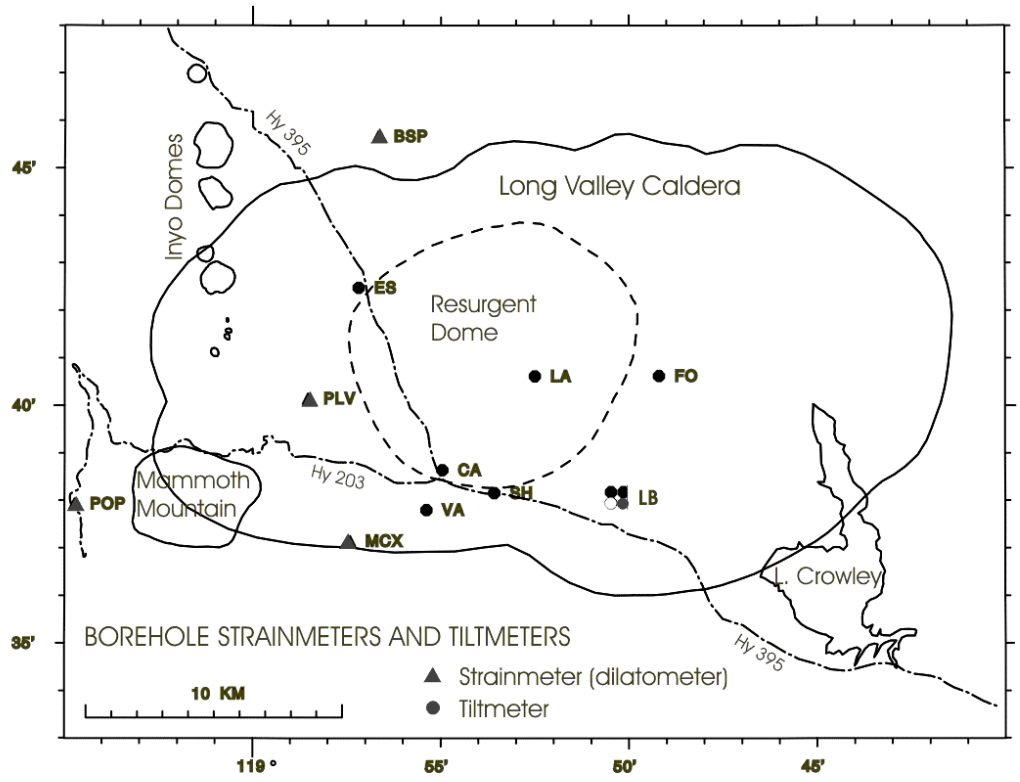

.

Figure D1. Locations of dilatometers and tiltmeters.

Highlights

The data during this year has been relatively quiet at all sites. Pressure corrected data are shown in Figures D2, A) and B). Comparative pore pressure data at the Postpile dilatometer site and the Big Springs dilatometer site is shown in Figure D2 C). Postpile continues to show gradual decrease in compression compared to the 1990's. The long term record is shown in D2 D). Some hint that the sense of strain at POPA has changed from compression to extension is apparent since 2008.

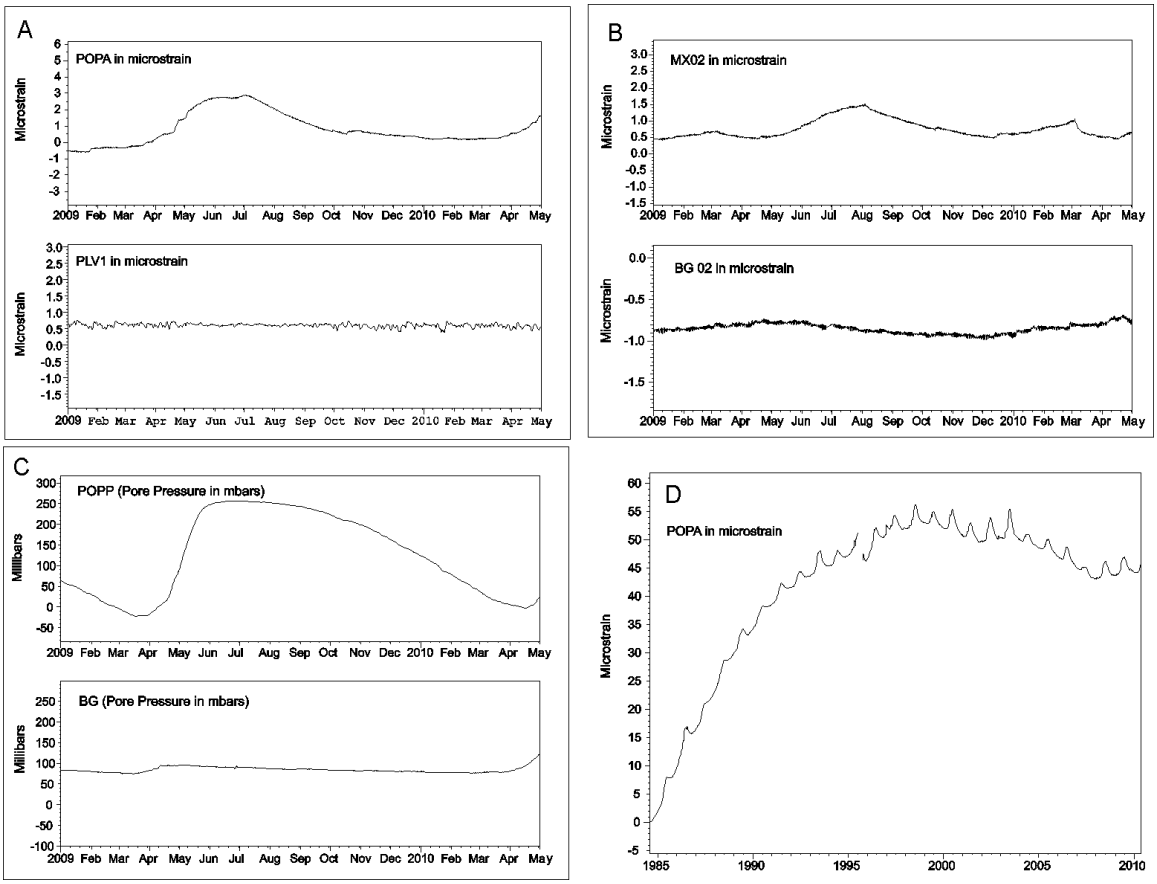

Figure D2: Borehole strain in Long Valley Caldera. A) POPA and PLV1 for 1 January 2009 – 1 May 2010. B) MX02 and BG02 for 1 January 2009 – 1 May 2010. C) POPA and BG pore pressure for 1 January 2009 – 1 May 2010. D) POPA strain for 1 August 1984 – 3 May 2010.

TILT MEASUREMENTS (Mal Johnston, Roger Bilham, Doug Myren and Stuart Wilkinson)

Instrumentation

Instruments recording crustal tilt in the Long Valley caldera are of two types - 1) a long-base (LB) instrument in which fluid level is measured in fluid reservoirs separated by about 500 m and connected by pipes, which was constructed by Roger Bilham of the University of Colorado, and 2) borehole tiltmeters that measure the position of a bubble trapped under a concave lens. For tiltmeter locations, see Figure D1. Real time plots of the data from these instruments can be viewed at http://quake.wr.usgs.gov/QUAKE/longv.html.

All data are transmitted by satellite to the USGS headquarters in Menlo Park, CA. Data samples are taken every 10 minutes. Plots of the changes in tilt as recorded on each of these tiltmeters are shown in Figures T1-T3. Removal of re-zeros, offsets, problems with telemetry and identification of instrument failures is difficult, tedious and time-consuming task. In order to have a relatively up-to-date file of data computer algorithms have been written that accomplish most of these tasks most of the time. Detailed discussion or detailed analysis usually requires hand checking of the data. Flat sections in the data usually denote a failure in the telemetry. Gaps denote missing data. All instruments are scaled using tidally generated scale factors.

Highlights

Fig T1 shows the long base data from Jan 1, 2009 to May 31, 2010. No changes of note are apparent except for a small overall net tilt down to the NW consistent with continued deflation and indications of an annual signal probably from meterological loading. Data from the short base tiltmeters are shown in Figures T3-T10. Very little of geophysical interest occurred this period. Data from the tiltmeters in the deep boreholes at Big Springs and Motorcross are shown in T8 and T9.

.

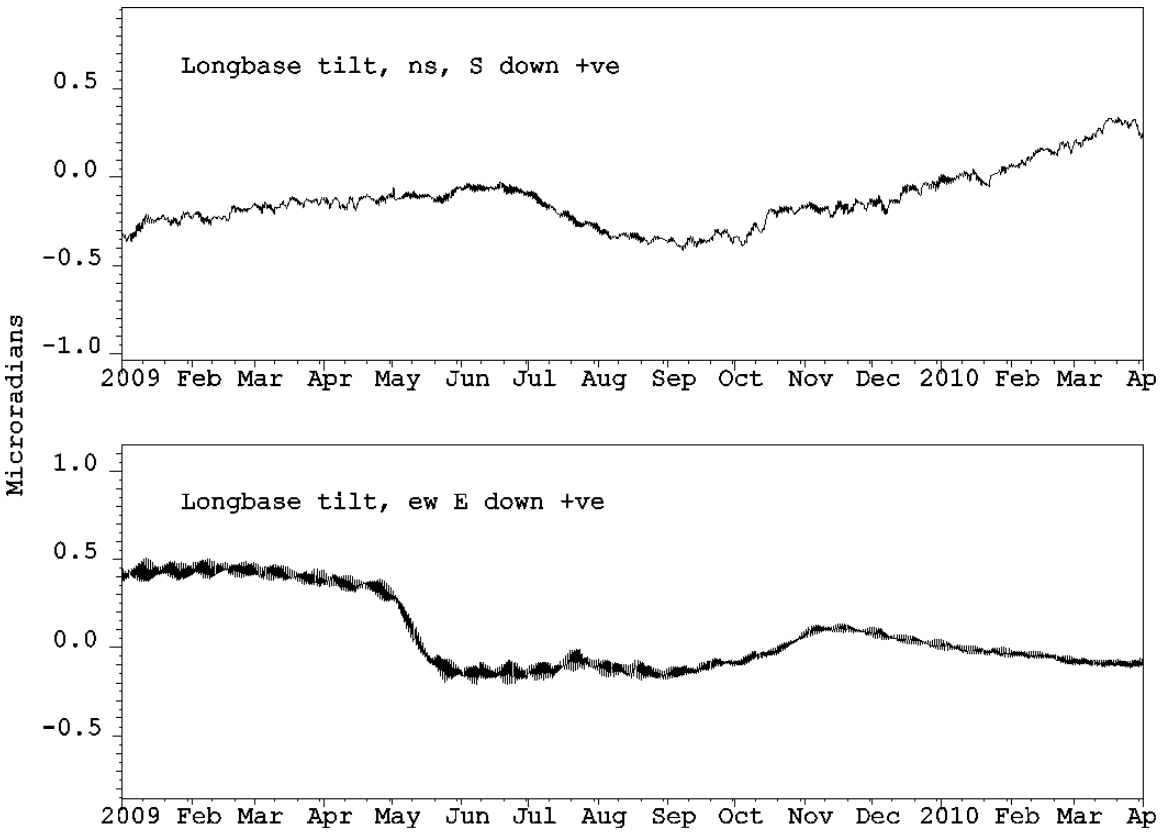

Figure T1. East-west and north-south components of the long-base tiltmeter for 1 January through 31 May 2010. Positive slopes indicate tilt down the south and east, respectively. Units in microradians.

.

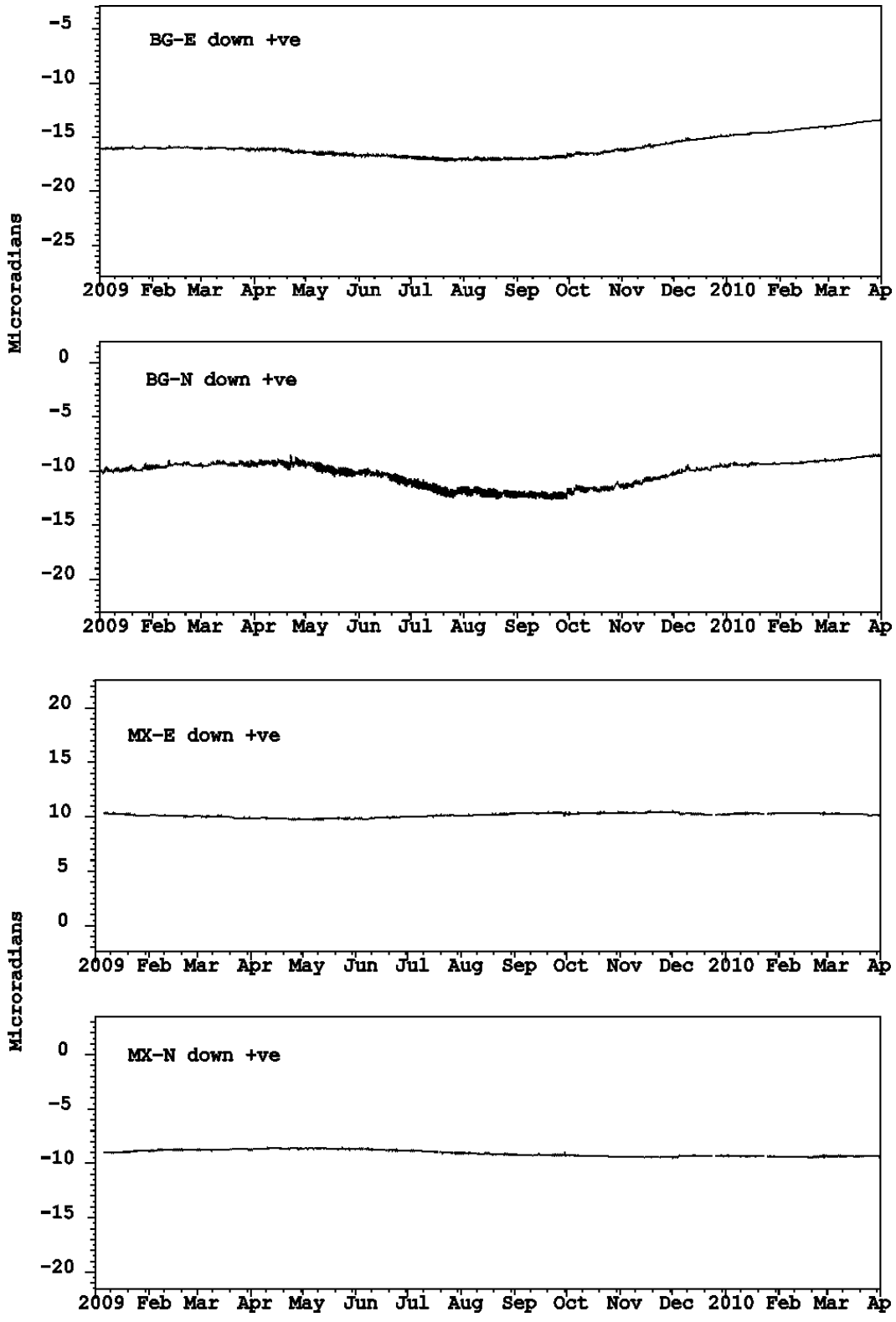

Figure T2. East-west and north-south components for the borehole tiltmeters installed with the Big Springs (BS) and Motocross (MX) dilatometers for June – December 2008. Units in microradians.

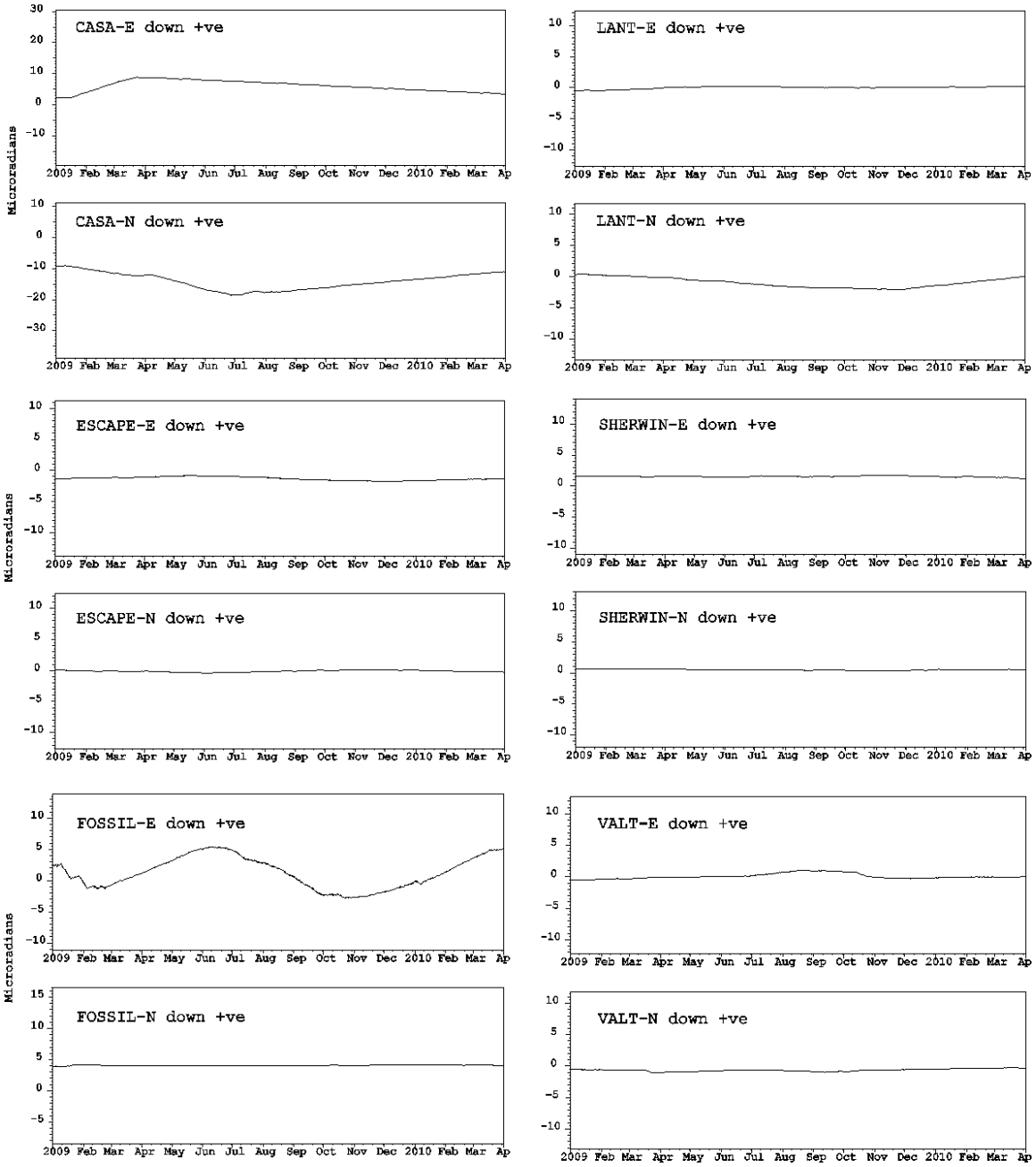

Figure T3. East-west and north-south tilt components for the shallow borehole tiltmeters for 1 January 2009 – 31 May 2010. Units in microradians.

MAGNETIC MEASUREMENTS (M.J.S. Johnston, S. Wilkinson, Doug Myren, Y. Sassai, and Y. Tanaka)

BACKGROUND

Local magnetic fields at 18 sites in the Long Valley Caldera are transmitted via satellite telemetry to Menlo Park every 10 minutes. These and other data provide continuous 'real-time'

monitoring in this region through the low-frequency data system. The location of these sites is shown on Figure M1. Temporal changes in local magnetic field are isolated using simple differencing techniques.

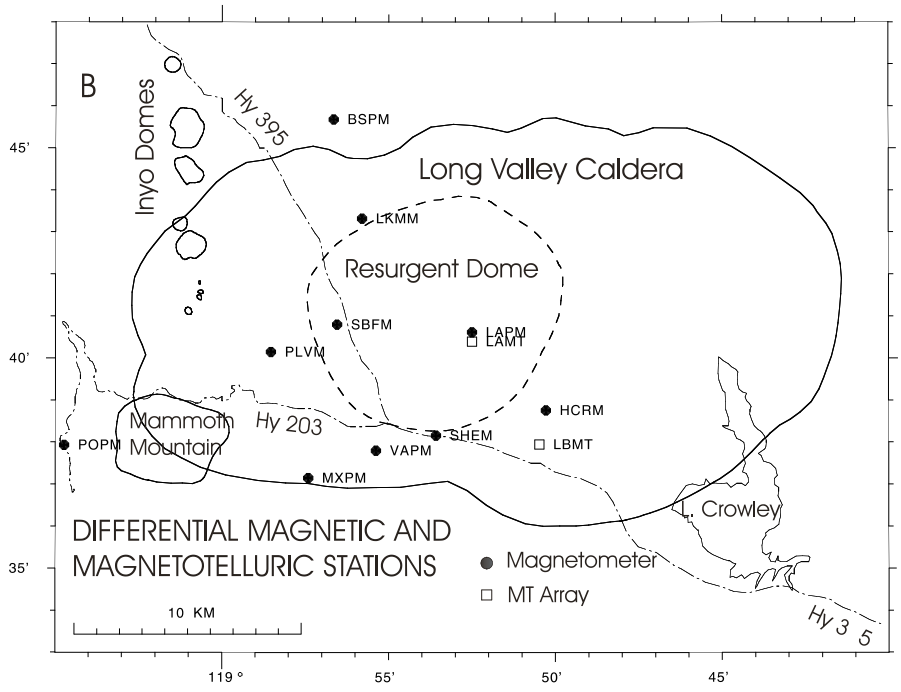

Figure M1. Locations of differential magnetic field stations within Long Valley caldera. The reference station MGS (not shown) is located along Highway 395 approximately 20 km southeast of the caldera.

DATA:
Plots of daily averaged data from the telemetered magnetometer stations in and near the caldera are shown in Figures M2.. As these instrument are getting old we are having great difficulty keeping them alive. Dedicated work by Stuart Wilkinson is greatly appreciated.

HIGHLIGHTS::
Nothing unusual during 2009.

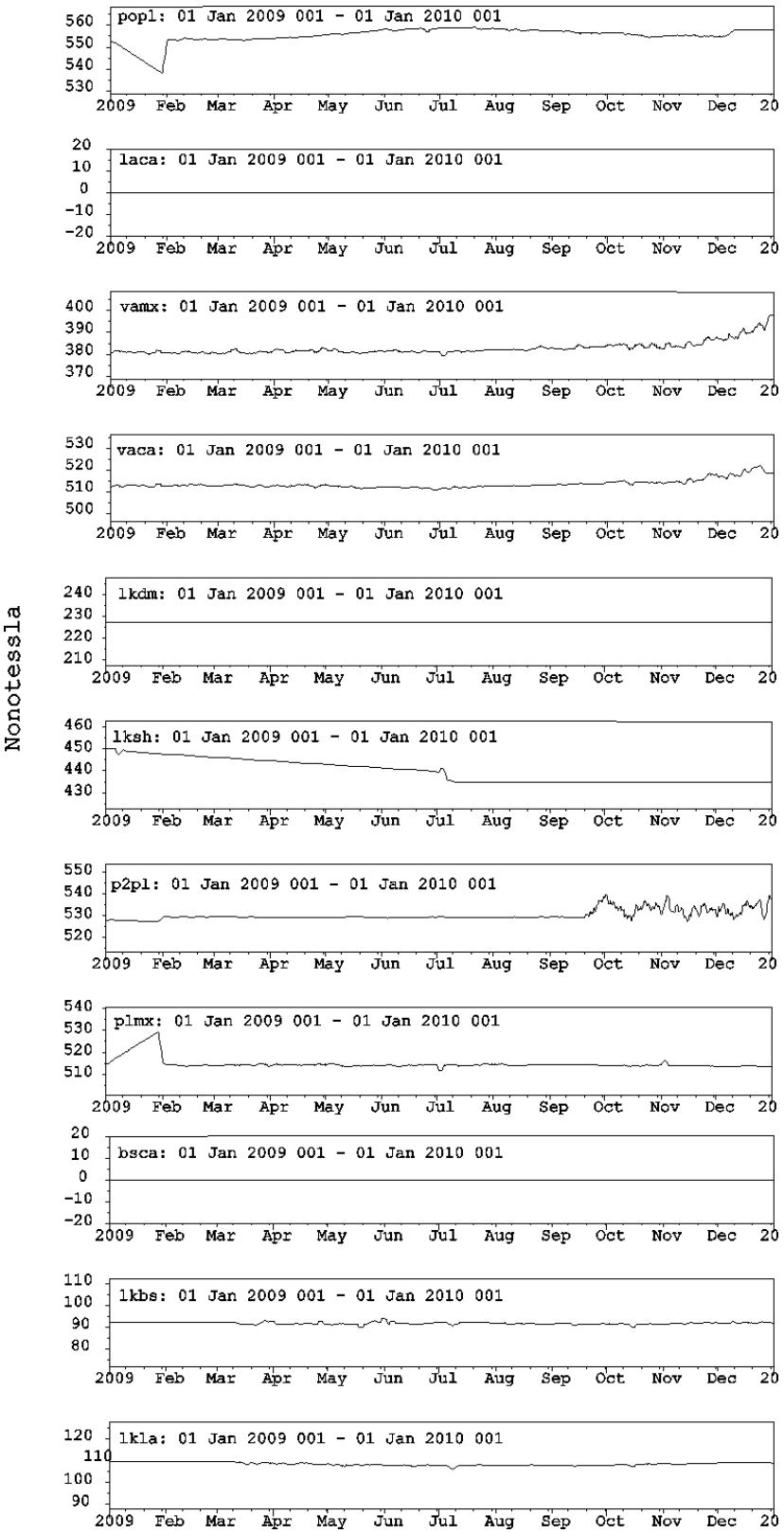

Figure M2. Differential magnetometer data for the stations shown in Figure M1: 2009.

CO_2 STUDIES - 2009

HORSESHOE LAKE TREE-KILL AREA (Cindy Werner, Mike Doukas, Peter Kelly, Volcano Emissions Project (VEP), Cascades Volcano Observatory, Vancouver, WA)

VEP maintains a CO_2 sensor network at Horseshoe Lake and also measures an array of points for CO_2 flux each year. Results of the 2009 data are summarized below.

Continuous CO_2 stations:

Station HS1 is located near the central portion of the Horseshoe Lake tree kill in an area of high CO_2 ground flux and has both a 0-100% sensor and a 0-50% CO_2 sensor (only data for 0-100% shown). Station HS2 is located in a lower flux area near the margin of the tree kill (not shown) and HS3 is at the edge of the tree-kill zone in the group campground area (also not shown). Stations HS2 and HS3 were not functioning when visited in 2009. Only one station is located away from Horseshoe Lake include SKI, located near the former Chair 19 in the Mammoth Mountain Ski Area (also not shown and not working). Due to non-operational sensors and disabled telemetry, the sites are going to be redesigned in the near future (2010-2011). The power was turned off at Horseshoe lake during the winter of 2009, thus no measurements will be recorded during that period. As of March 2010, power was still off.

At all sites, CO_2 collection chambers are buried in the soil. Air from these collection chambers is pumped to nearby carbon dioxide sensors housed in USFS structures or culverts. Local barometric pressure is also measured at HS1 using a Vaisala Pressure Transducer. Data were collected from the sensors every hour and logged onsite for downloading. Snow data were obtained from a U.S. Bureau of Reclamation monitoring station at Mammoth Pass

CO_2 data for 2009 for are shown below along with air temperature and snow depth at Mammoth Pass. [**Note: Data not corrected for pressure and temperature.**] The typical annual buildup of CO_2 at Horseshoe Lake as seen most years was visible in this year. No increase in CO2 was observed with the increase in seismicity in September 2009.

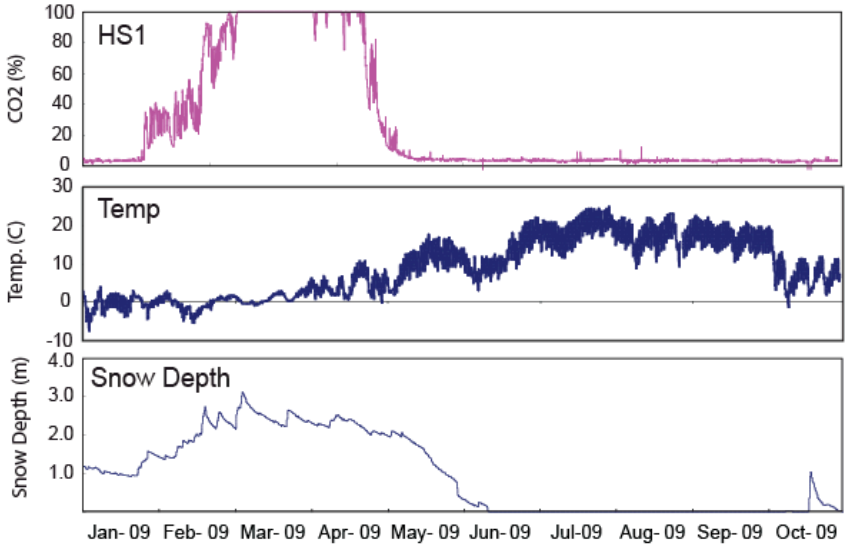

CO_2 flux survey:

During the annual monitoring station servicing trip to Long Valley in August, CVO gas project personnel also conducted their annual soil CO_2 efflux survey at Horseshoe Lake. The results are shown below. The long term degassing rate average through 2005 had been about 100 tons of CO_2 per day at Horseshoe Lake. The rate measured in August 2009 was also near 100 t/d (107 t/d), slightly up from 2008 when emissions were on the order of 100 t/d.

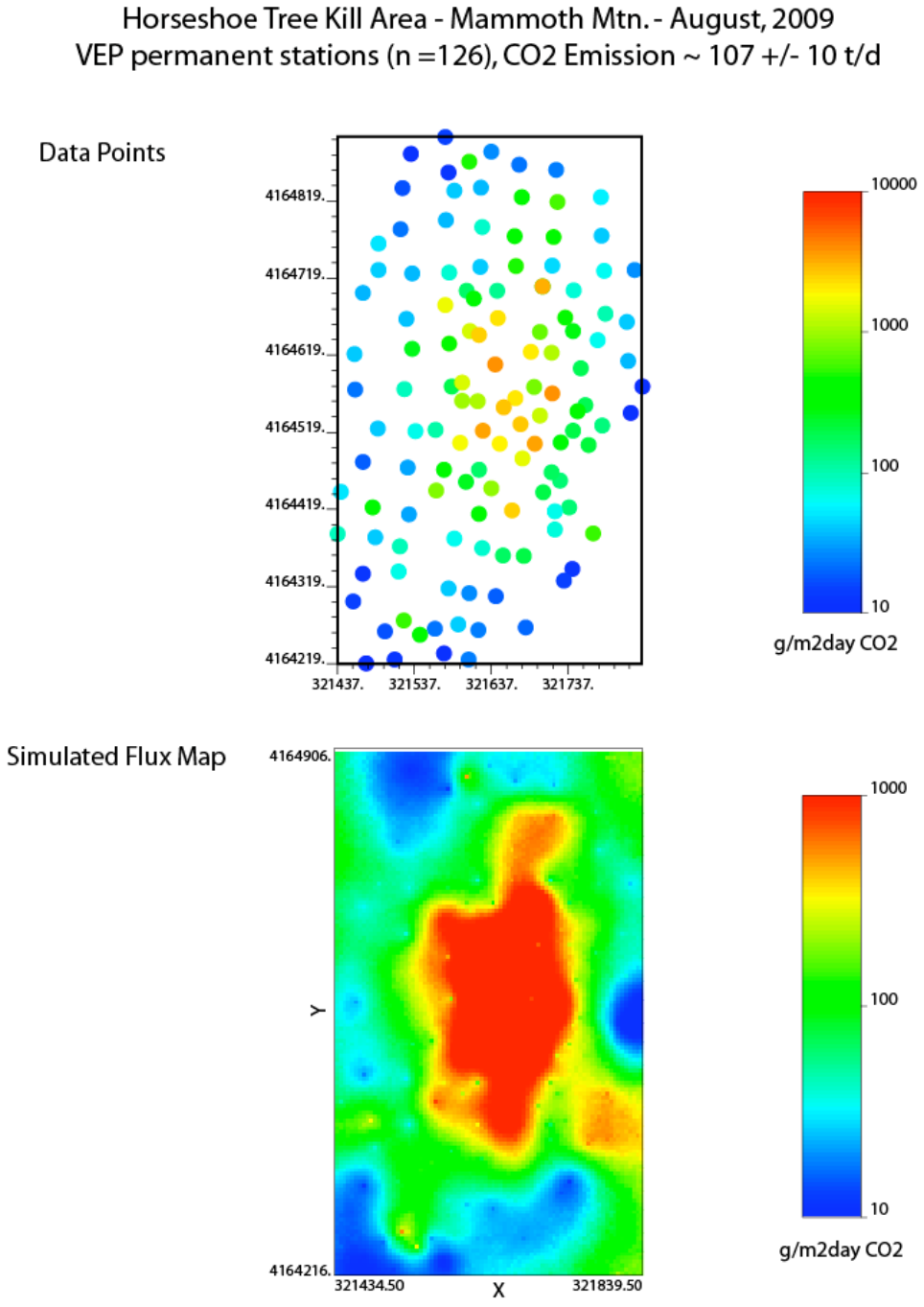

CARBON DIOXIDE STUDIES AT MAMMOTH MOUNTAIN: Christopher Farrar, U.S. Geological Survey, Carnelian Bay, CA

Background

Field surveys to measure and assess changes in carbon dioxide emissions from Mammoth Mountain were carried out during September 2009. Known CO_2 emission areas on Mammoth Mountain form a discontinuous ring around the south, west, and north sides of the mountain at altitudes between 2,700 and 3,000 meters. The largest areas emit CO_2 at ambient air temperatures diffusely from soils (sites HSL, RC, and CH-12 in fig cf-1). A few smaller areas of CO_2 emission, on the north and south flanks of the mountain, are associated with thermal ground and identifiable steam vents (MMF and SSF in fig cf-1). Measurements have been made annually at HSL for over a decade; more complete surveys that include HSL, RC, and CH12 have been made annually since 2005 (table cf-1). Measurements in the two thermal areas have been less frequent. Prior to 2008, the last complete survey in SSF area was made in 1996.

CO_2 emissions at over 600 stations were calculated from ground-based measurements of changes in CO_2 concentration in closed chambers (volume approximately 4 liters) over intervals from 1 to 3 minutes. CO_2 concentrations in the chambers were measured using infrared non-dispersive gas analyzers. Locations of measurement sites were determined with hand-held GPS receivers (generally precise to about 10 m). Total CO_2 flux from each area, expressed in tonnes per day (t/d), was estimated from grids of evenly spaced data produced by a Kriging interpolation routine run on the measured values.

Results

The results of the measurements made in 2009 are compared to similar measurements made in 1996 and 2005-2008 in table cf-1. Estimates of total CO_2 emission from the five sites on Mammoth Mountain based on data collected in 2009 are similar to the estimates made for 2005-2008. The total (not including Southside area) estimated for 2009, 84 t/d, is the highest for the years 2005-2009 but far lower than estimates from 1996. The differences in total emissions from the three largest areas (HSL, RC, CH12) between years 2005-2009 are not large (about 22 % of the mean of 76 t/d). Such differences may be related to variations in near surface conditions and may not signify changes in gas release from the source, several kilometers beneath the mountain. Variations in atmospheric conditions (pressure and wind), soil-moisture, the development of winter snowpack and melting, ground-water recharge and movement all can influence gas emissions from the soil. Also part of the differences in estimated emissions relate to slightly different boundaries used in the surveys between years.

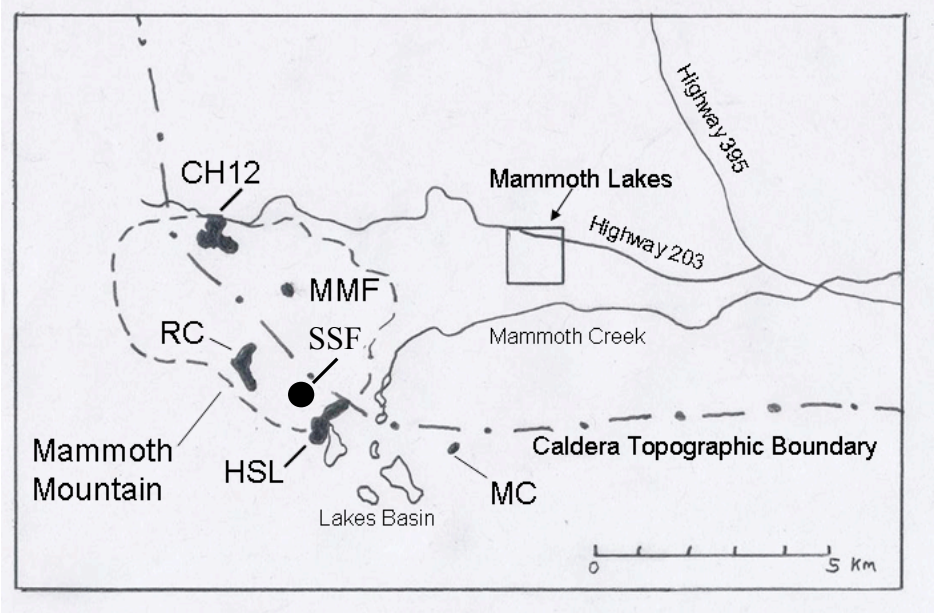

Figure cf-1. Locations of Carbon Dioxide Measurements

CF-1. Mammoth Mountain CO_2 Flux Summary

Values in tones/ day

Location	1996	2005	2006	2007	2008	2009
Horseshoe + Borrow Pit	**134**	**40.1**	**22.2**	**27.2**	**46.0**	**26.8**
Chair 12	**48**	**17.4**	**13**	**24.6**	**17**	**28.4**
Reds Creek	**308**	**23.8**	**23.6**	**22.4**	**18.4**	**27.1**
Southside[1]	**5**	**--**	**--**	**--**	**12**	**7**
MMF	**6**	**--**	**1.6**	**2**	**1.9**	**2.2**
Total[1]	**501**	**81**	**60**	**76**	**83**	**84**

([1] flux from Southside not included)

CO_2 EMISSIONS STUDIES (Deborah Bergfeld, William Evans and Chris Farrar).

Background on 2009 Field Studies

Field studies of CO_2 emissions during 2009 focused in part on monitoring the flux of CO_2 from established grids, as well as starting new research to quantify CO_2 discharge at the Mono Craters water tunnel. Our early work to quantify diffuse CO_2 emissions on the resurgent dome began in late 2002 and present day configurations of the monitoring sites were defined in 2006. CO_2 emissions studies along the Mono Craters volcanic chain began in 2007. Summary statistics of flux measurements since 2006 are provided in Table 1.

The 2009 CO_2 monitoring studies were performed in July at Basalt Canyon (BSLT) and Shady Rest (SRST), two areas of vegetation-kill on the resurgent dome, and in June, at North Coulee (NC), a glassy rhyolite flow in the northern portion of the Mono Craters volcanic chain (Fig. 1). CO_2 flux measurements were made using an accumulation chamber coupled with an infrared CO_2 analyzer. Soil temperatures were measured at a targeted depth of 20 cm at BSLT and SRST and were not measured at NC. CO_2 flux is reported as grams of CO_2 per meter squared per day (g $m^{-2}d^{-1}$). The average flux at each grid is calculated using a sequential Gaussian simulation of the measured CO_2 flux using GSLIB statistical software. Total CO_2 emissions reported as metric tonnes of CO_2 per day (t d^{-1}), are calculated from the average flux multiplied by the grid area.

A pilot study of CO_2 emissions from the east portal of the Mono Craters water tunnel took place on June 23, 2009. Access was granted by the Los Angeles Department of Water and Power (LADWP). Dangerously-high CO_2 concentrations prevented us from entering the tunnel interior and all work was performed at the mouth of the tunnel. Water samples for dissolved carbon were collected from the stream at the point where it leaves the tunnel. The stream discharge was provided by the LADWP gage. Air flow (wind speed) coming out of the tunnel was measured by suspending a digital anemometer from a cross bar, about a meter from the top of the tunnel. Intake tubing for the CO_2 analyzer was attached to the pole holding the anemometer. The same set up was used to collect 2 gas samples at the end of the experiment. Wind speed and CO_2 concentrations were measured for about 90 minutes beginning at 9:30 a.m. We ended the test when turbulence from cross winds outside of the tunnel compromised our ability to make measurements.

Long Valley Caldera, Resurgent Dome

Irregular growth patterns and vegetation kills at BSLT and SRST provide visible evidence of thermal fluid upflow. At both sites the size of the kill zone is growing, but due to the possibility of insect-kills the cause of mortality is not confirmed. During 2009, as in past years, we increased the footprint and the number of measurement sites at both grids. In addition, we discovered a small localized area of vegetation kill that falls along a trend between the SRST grid and the Casa 66-25 geothermal production well (Fig. 1 inset). CO_2 flux and soil temperatures were measured at 12 sites in this new area. The maximum flux and soil temperature were recorded at the same site and were 156 g $m^{-2}d^{-1}$ and 49.7 °C, respectively. If the kill area continues to grow we will incorporate it into the SRST grid.

In order to compare temporal changes in emissions data we have designated *core* measurement sites for the BLST and SRST grids. The core sites are defined as locations where flux measurements have been made on at least 80% of the site visits. Core sites at BSLT and SRST cover 15,000 m^2 and 58,000 m^2, respectively. Results from these sites since 2006 show that total

CO_2 emissions were somewhat elevated at SRST in June 2007, but for the most part, emissions from both grids are essentially static over time (Table 1).

Mono Domes, North Coulee

Conditions at NC are unique in that there is no soil and essentially no vegetation grows around any of the measurement sites. As such, there are no sources for biogenically-derived CO_2, and any diffuse emissions of CO_2 can be considered anomalous. Carbon isotope and air-corrected helium isotope values from gas samples collected from high flux areas on NC are comparable with values obtained at Mammoth Mountain fumarole. However, maximum subsurface CO_2 concentrations at NC are around 5% compared to soil-gas CO_2 concentrations that are > 95% at Mammoth Mountain.

The lack of vegetation and other visible evidence of fluid upflow on NC has made it difficult to assess if we have discovered all areas with anomalous CO_2 emissions. Results from 2007–08 showed some correlation between areas containing bleached or reddish discolored rock outcrops with elevated CO_2 efflux. In June 2009 we measured subsurface CO_2 concentrations at several areas northeast of the main grid that contained outcrops of altered rocks. We found no evidence of anomalous CO_2 emissions at those locations. With those findings we stopped exploration for new sites at NC. Flux measurements were conducted over the established grid.

Results from the three flux surveys at NC are presented in Table 1. Average CO_2 flux values are around 40 g $m^{-2}d^{-1}$ and are much lower than the average CO_2 flux from the resurgent dome grids. Total CO_2 emissions from the NC grid are consistent over the span of this study and are around 10 t d^{-1}.

CO_2 Emissions from the East Portal, Mono Tunnel.

The east portal of the Mono tunnel has an arched top. Wind speed measurements showed there was a zone with no air flow about 2.5 feet from the top of the tunnel. Interestingly, throughout the morning swallows flew into the tunnel and their nests could be seen lining the roof in this zone. Presumably, CO_2 concentrations in this part of the tunnel were near background levels. The first measurements of wind speed and CO_2 concentration began at 9:30 a.m. For the next 30 minutes the wind speed out of the tunnel was relatively steady, ranging between 0.5 and 0.6 m s^{-1}, with CO_2 concentrations around 4 to 5%. From 10:00 to 10:30 wind speeds declined and CO_2 concentrations remained the same. Following this time period the measurements began to be influenced by cross winds. At 10:45 there were periods of time when the anemometer stopped and we discontinued the test at 11:00.

Estimates of total CO_2 emissions from the East portal tunnel include the dissolved flux of CO_2 in the stream, and the airborne flux based on wind speed. The dissolved flux is determined from the carbon content of the water multiplied by the discharge. Given a flow rate of 0.4 m^3s^{-1} results from our samples yield 8.6 t d^{-1} of dissolved CO_2. The tunnel CO_2 emissions are calculated using the area of the tunnel that had a measureable flow of gas, the average wind speed and average CO_2 concentration. During the first 30 minutes of the test emissions were about 13 t d^{-1}, and dropped to <5 t d^{-1} at the end of the experiment (Fig. 2).

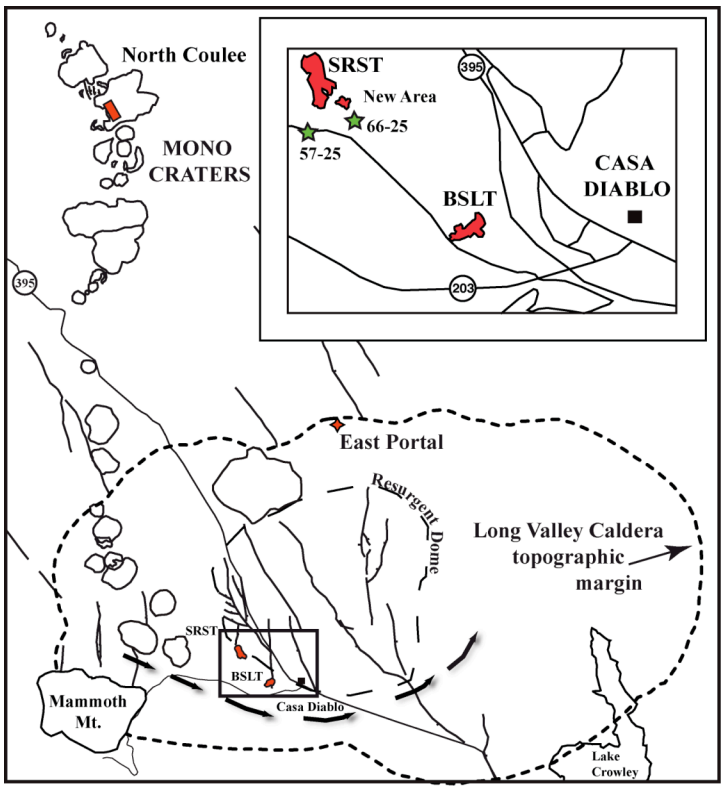

Figure 1. Location map showing flux grids (in red) at Shady Rest, Basalt Canyon and North Coulee. East Portal is the location of a pilot study initiated in 2009. Arrows around the resurgent dome indicate the flow main thermal aquifer. Rectangle shows area of the inset map. Green stars show locations for 2 geothermal production wells.

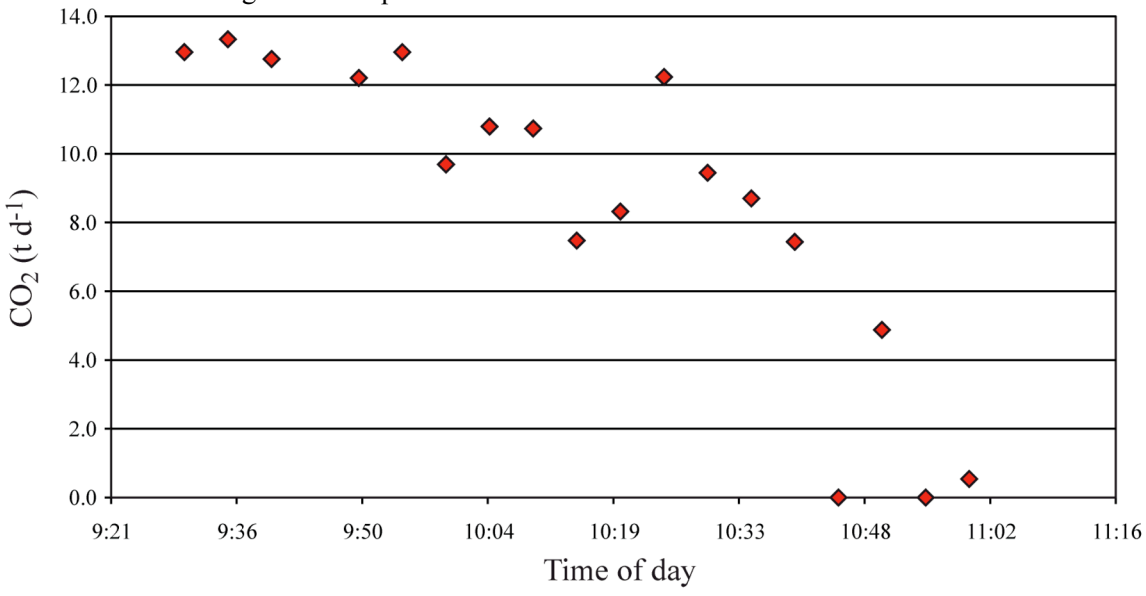

Figure 2. CO_2 emissions on June 23, 2009 from the East Portal of the Mono water tunnel.

BASALT CANYON					CORE SITES (15,000 m^2)		
Year	N	Area (m^2)	Avg flux ($gm^{-2}d^{-1}$)	Discharge (td^{-1})	N	Avg flux ($gm^{-2}d^{-1}$)	Discharge (td^{-1})
06 2006	66	14075	359	5.1	60	343	5.1
09 2006	64	13300	342	4.5	59	334	5.0
06 2007	83	19975	162	3.2	60	238	3.6
06 2008	83	17110	287	4.9	60	229	3.4
07 2009	85	22750	244	5.6	53	226	3.4
SHADY REST					CORE SITES (58,000 m^2)		
09 2006	81	58950	151	8.9	77	132	7.7
06 2007	90	64375	246	15.8	77	241	14.0
05 2008	105	75675	108	8.2	77	124	7.2
07 2009	106	80250	145	11.6	77	162	9.4
NORTH COULEE					ALL SITES* (240,000 m^2)		
06 2007	206	204875	38	7.8	206	38	9.1
06 2008	174	253150	39	9.9	174	39	9.4
06 2009	140	255775	44	11.3	140	44	10.6

Table 1. Summary statistics since 2006 for CO_2 emissions at Basalt Canyon and Shady Rest grids on the resurgent dome, and since 2007 for North Coulee in the Mono Craters volcanic chain. Data for core sites as described in text. Emissions for all sites (*) on NC are calculated assuming a 240,000 m^2 area.

HYDROLOGIC MONITORING (*Chris Farrar and Michelle Sneed: U.S. Geological Survey, Carnelian Bay and Sacramento, CA).*

Hydrologic data collected for the USGS Volcanic Hazards Program in this report include ground-water level data from four wells; stream flow, water temperature, and specific conductance from one site on Hot Creek; and estimated thermal water discharge in Hot Creek Gorge (figure H1). Additional data are available on the web at -- http://lvo.wr.usgs.gov/HydroStudies.html or upon request – contact: *Chris Farrar at Carnelian Bay 530.546.0187.*

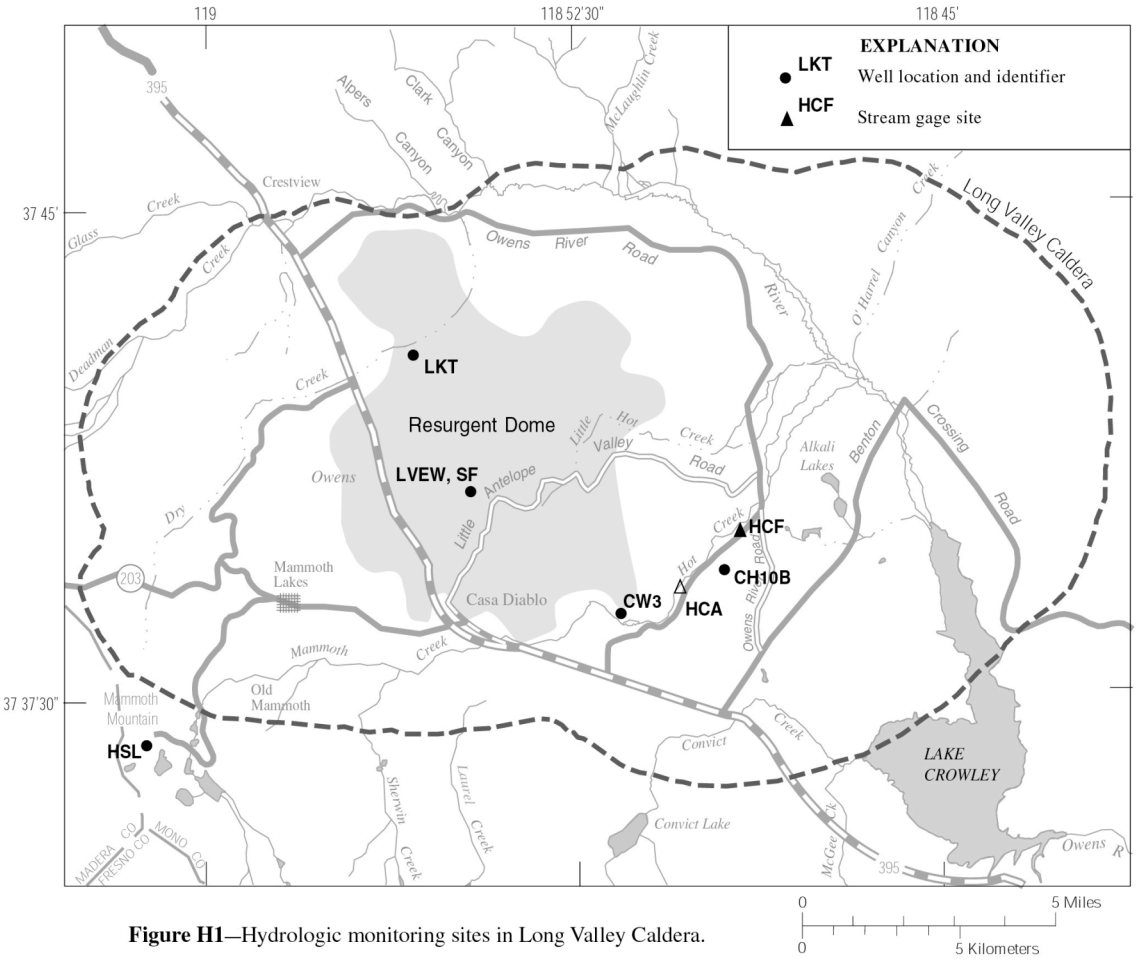

Figure H1—Hydrologic monitoring sites in Long Valley Caldera.

BACKGROUND

Ground-water levels in wells and the discharge of springs can change in response to strain in the Earth's crust. The network of wells and surface water sites provides hydrologic data that contributes to monitoring deformation and other changes caused from magmatic intrusions and earthquakes in Long Valley Caldera.

GROUND-WATER LEVEL MONITORING

Ground-water levels are measured continuously in four wells, LKT, LVEW, SF, and CH-10B (locations in figure H1), using pressure transducers that are either submerged below the water surface or placed above ground and sense back-pressure in a nitrogen-filled tube extending below the water surface. Barometric pressure is also measured at each site using pressure transducers. The data are recorded by on-site data loggers and telemetered on a three-hour transmit-cycle using the GOES satellite and receivers at Menlo Park and Sacramento. All sites are visited monthly to collect data from on-site recorders and to check instrument calibrations.

Data processing is done in the Sacramento Office. Records of barometric pressure are used in combination with the water-level records to determine aquifer properties from the observed water-level response to atmospheric loading and earth tides. The influences of barometric pressure changes and earth tides are removed from the water-level records. The result yields the filtered water-level record that may contain other hydraulic and

crustal deformation signals. Filtered data for wells LKT and CH-10B are given in figures H2 and H3.

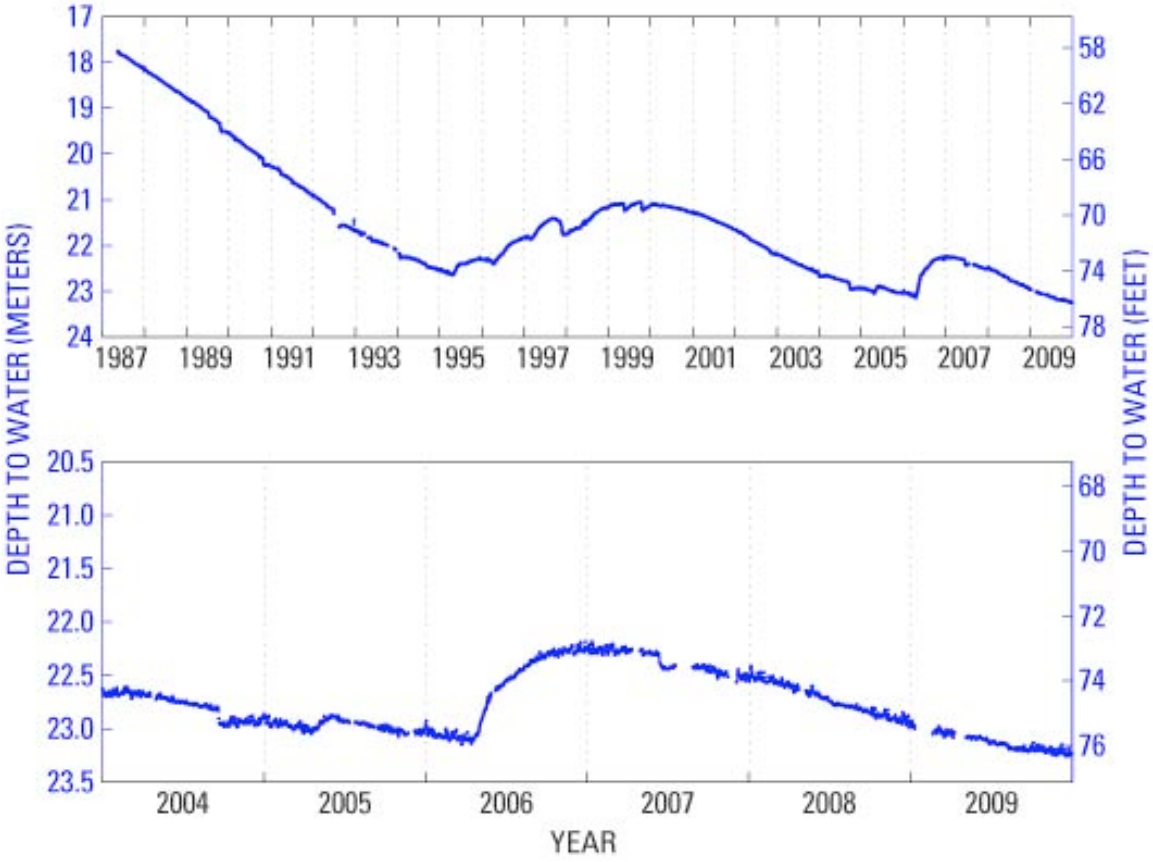

Figure H2. Hydrographs for well LKT, based on filtered daily mean values. The rise, beginning in mid-2006 is from a strong recharge pulse derived from the above average winter 2006 snow-pack. The decline in level that began in 2007 continued through 2009 because of minimal recharge in the northwest part of the caldera.

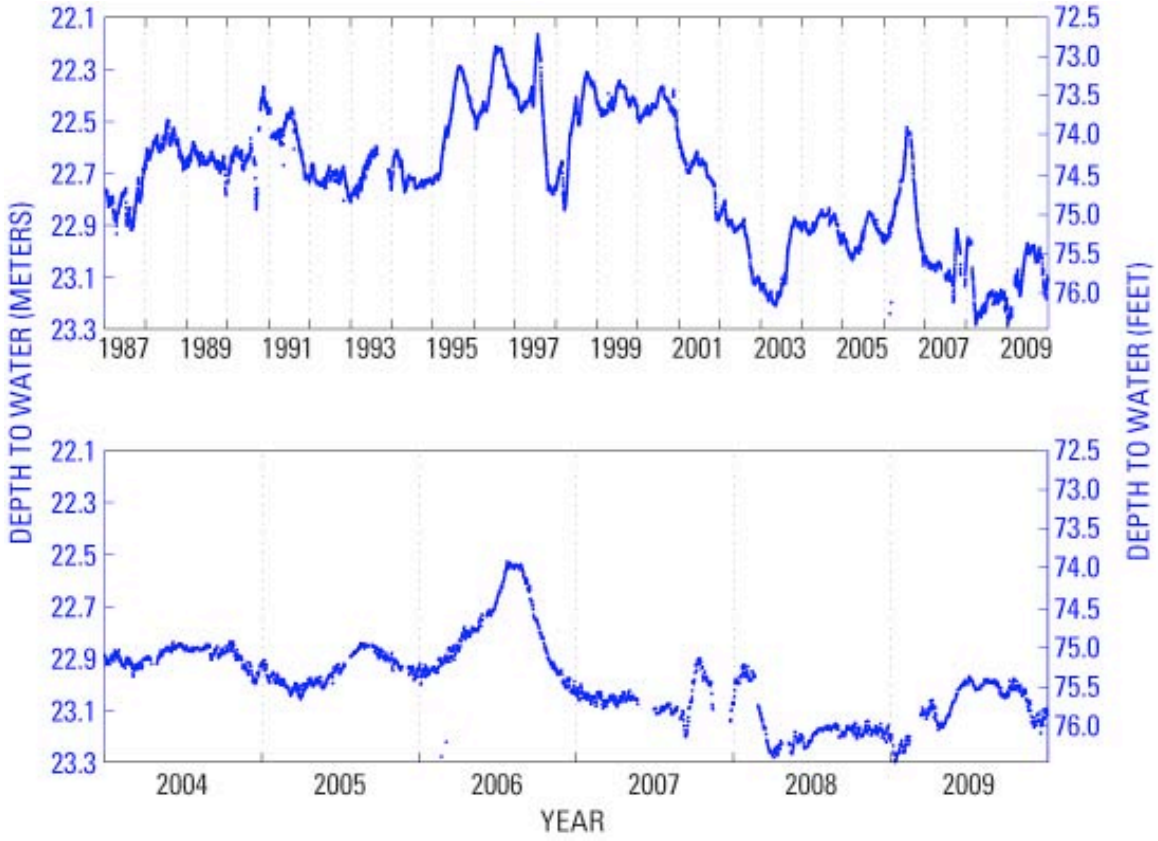

Figure H3. Hydrographs for well CH10B, based on filtered mean daily fluid levels. The large fluid level rise in mid-2006 is due to high recharge from above average precipitation during the winter of 2006. The fluid level oscillated about 0.2 m during the last half of 2007 and first part of 2008. The oscillations in level are consistent with some of the shifting in locations of thermal spring discharge in Hot Creek Gorge. In March 2008, after reaching the lowest water level in 21 years of observation, the level rose through most of 2009 and began a modest decline in autumn 2009.

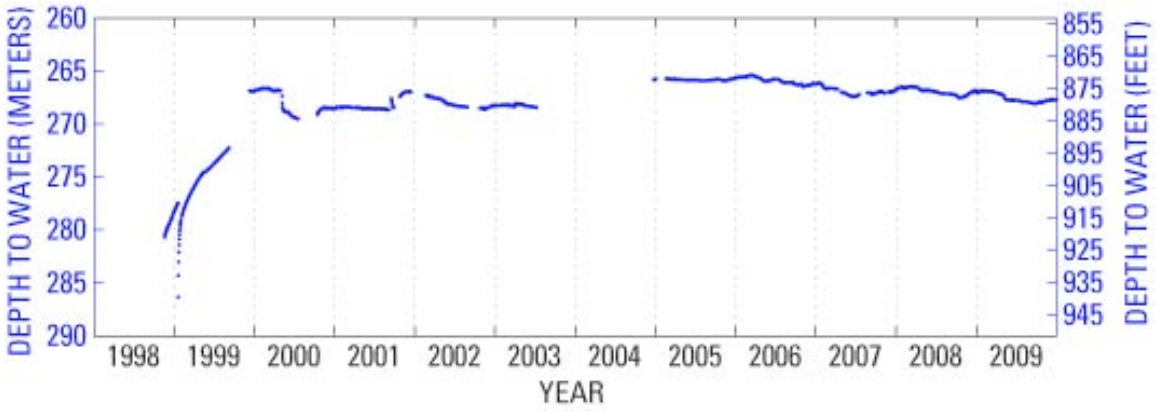

Figure H4. Unfiltered fluid levels in well LVEW.

The fluid level in well LVEW is controlled by the pressure in a fractured rock aquifer at a depth of about 3000 m below land surface and therefore is largely buffered against seasonal fluctuations. The early records from 1998-99 are strongly affected by well testing. The fluid level has declined variably through 2009 from the high levels of 2004.

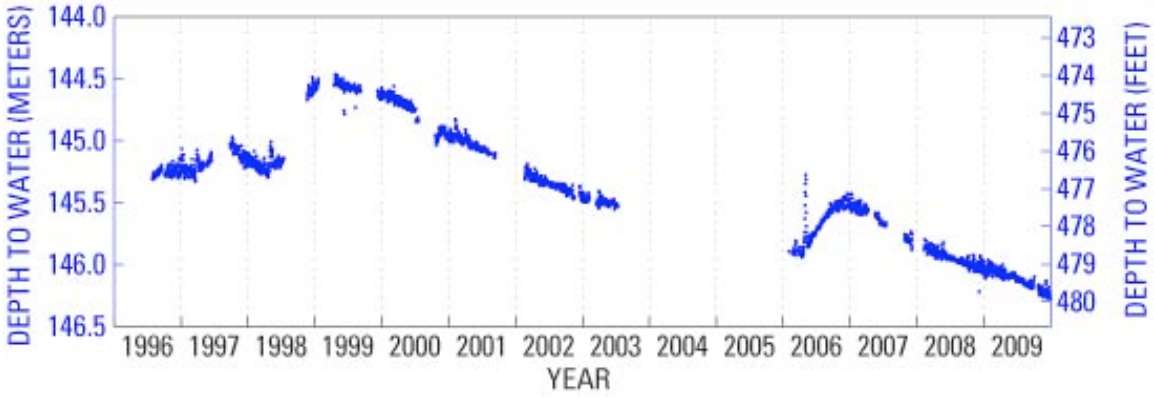

Figure H5. Unfiltered fluid levels in well SF, near LVEW.

The fluid level in well SF represents the hydraulic pressure in the upper 270 m of volcanic rock making up the resurgent dome. Fluid levels in SF respond to inter-annual patterns of precipitation and recharge. The fluid level has dropped from early 2007 to 2009, reaching its lowest level in 14 years of observation.

SURFACE WATER MONITORING

Site HCF is located downstream from the thermal springs in Hot Creek Gorge (figure H1). Stage, water temperature, and specific conductance (figure H6) are recorded every 15-minutes. The data are recorded by an on-site data logger and telemetered every three hours. Specific conductance is a measure of total dissolved ionized constituents. Water at HCF is a mixture of thermal water from springs along Hot Creek and non-thermal water from the Mammoth Creek basin. Changes in specific conductance are related to changes in the mixing ratio of thermal and non-thermal components of stream flow. Water temperatures change in response to ambient temperatures and the mixing ratio.

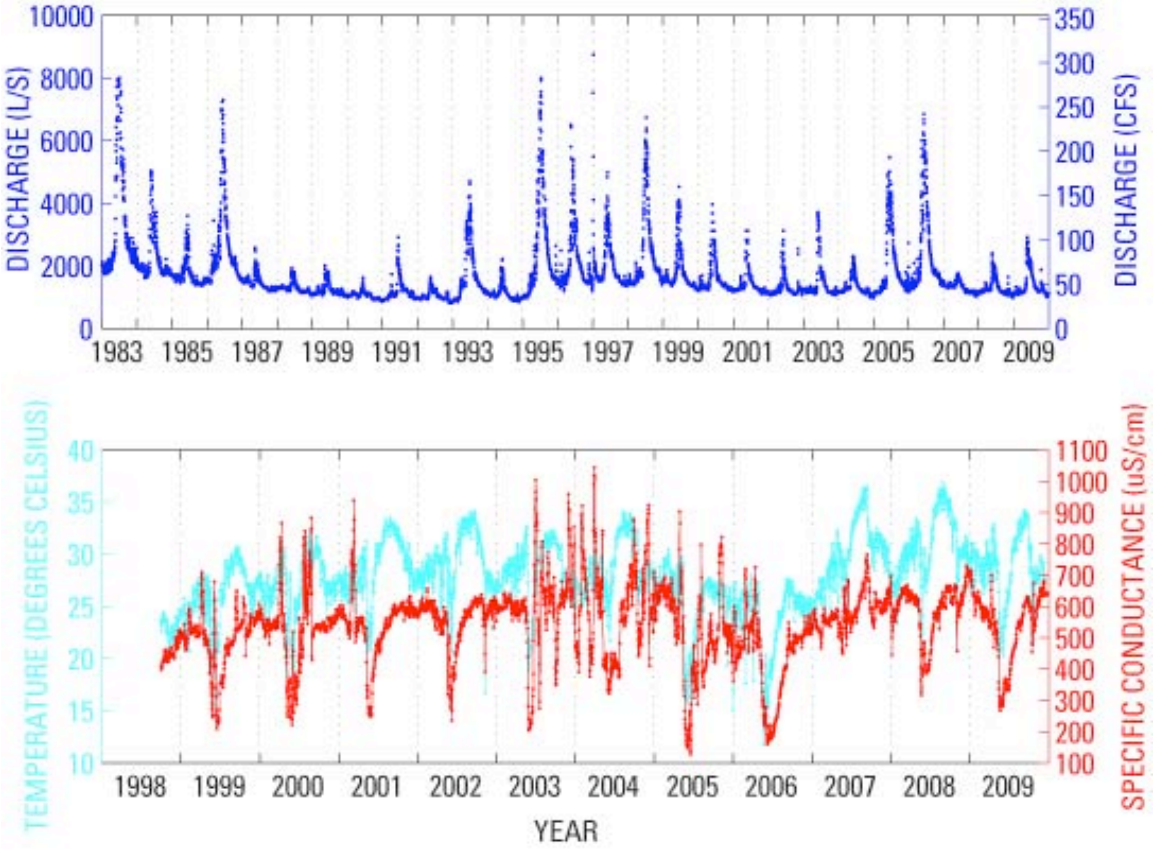

Figure H6. Discharge, water temperature, and specific conductance at Hot Creek Flume (HCF), based on daily mean data.

The effects of back to back winters with below average precipitation can be seen in the very small discharge peaks during spring runoff in 2007 and 2008. Discharge increased slightly in 2009. The relatively high water temperatures and specific conductance throughout 2007-2009 are the result of low discharge and higher proportion of thermal water.

THERMAL WATER DISCHARGE ESTIMATE

Estimates of total thermal water discharge (figure H7) are computed from monthly measurements of discharge, and boron and chloride concentrations collected at a non-recording site (HCA) located upstream of the Hot Creek gorge thermal area and at site HCF downstream. The quantity of thermal water discharged to Hot Creek is known to vary in response to seasonal variations in precipitation, snow-melt, earthquakes, and other processes. It is believed that spring discharge may change in response to crustal strain.

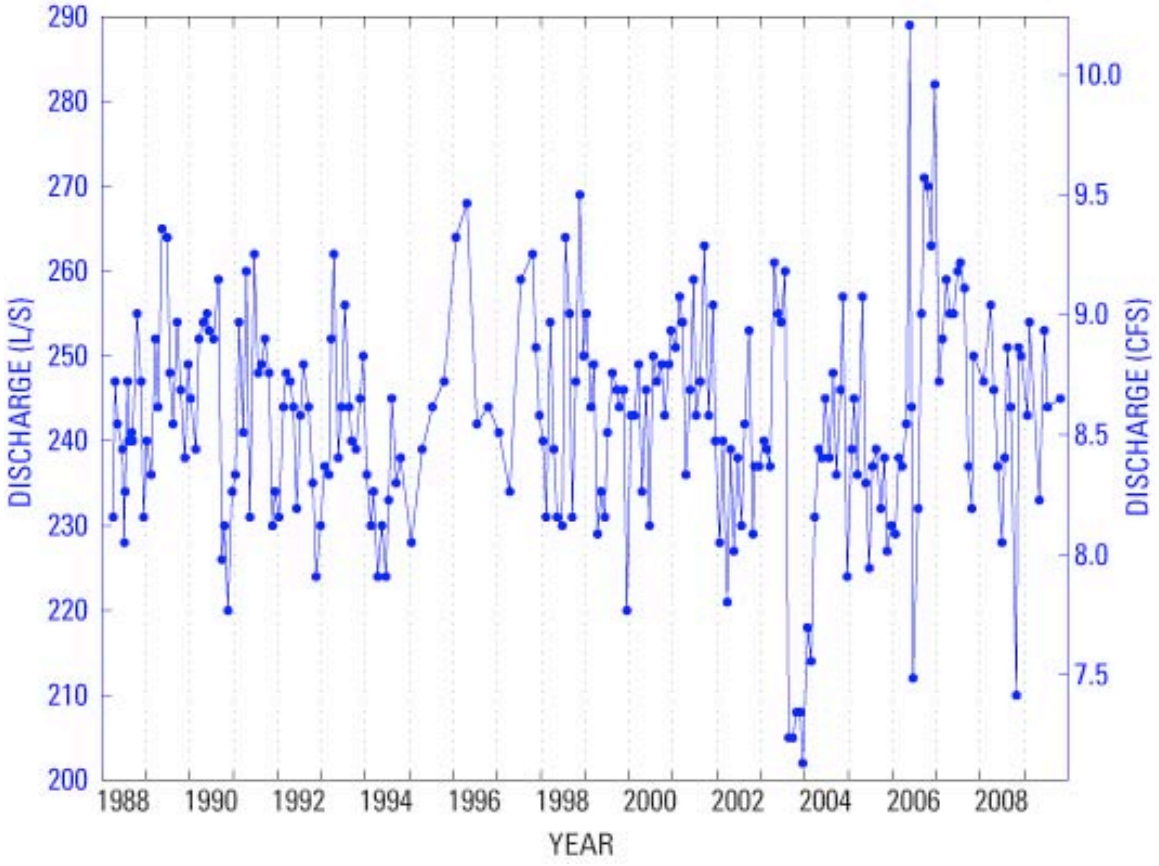

Figure H7. Estimated thermal water discharge for springs in Hot Creek Gorge.

Thermal springs in Hot Creek Gorge have continued to exhibit variability in discharge, temperatures, and vent locations throughout 2009. The vigorous fountaining-discharge from springs that began in May 2006 and continued into 2007 has been more subdued and infrequent in 2009. The mean estimated total thermal water discharge of 245 L/s for 2009 is slightly less than the mean of 251 L/s for 2006 and 2007. In 2009 water temperatures in spring vents along the banks of Hot Creek were generally cooler than 2006-2008. Only a few small vents had temperatures near boiling (93 C) and maximum temperatures in the larger pools on the left bank were generally in the range 75-85 C. The U.S. Forest Service closure to swimming remains in effect because of the unpredictable behavior of the springs and areas of soil instability along the banks of Hot Creek.